Study of hyperon-nucleon interactions at BESIII

Jielei Zhang
(zhangjielei@ihep.ac.cn)

Henan University

Hadron Physics Online Forum (HAPOF)
https://indico.itp.ac.cn/category/5/

2025.05.09

Outline

- Introduction
- BEPCII and BESIII
- Study of hyperon-nucleon interactions at BESIII

  PRL 130, 251902 (2023)

  PRC 109, L052201 (2024)

  PRL 132, 231902 (2024)
- Summary

Scattering experiments of particle beams bombarding target materials

1911


Ernest Rutherford

$\alpha + \mathrm{Au}$

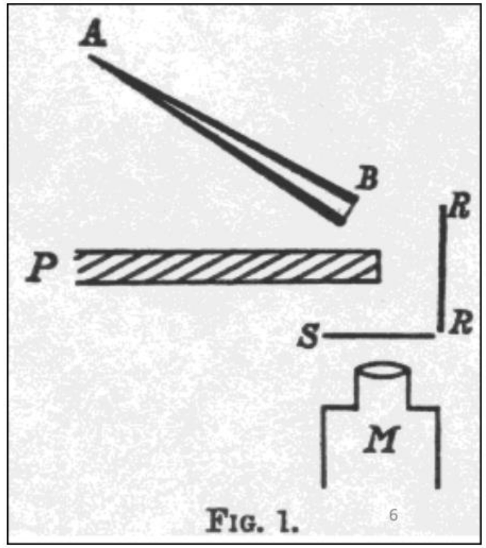

Nuclear structure model of atom

1919 $\alpha + \mathrm{N}$ Observation of proton

1932 $\alpha + \mathrm{Be}$ Observation of neutron


James Chadwick

Scattering experiments of particle beams bombarding target materials

1974

$p + \mathrm{Be} \rightarrow e^{+}e^{-}X$

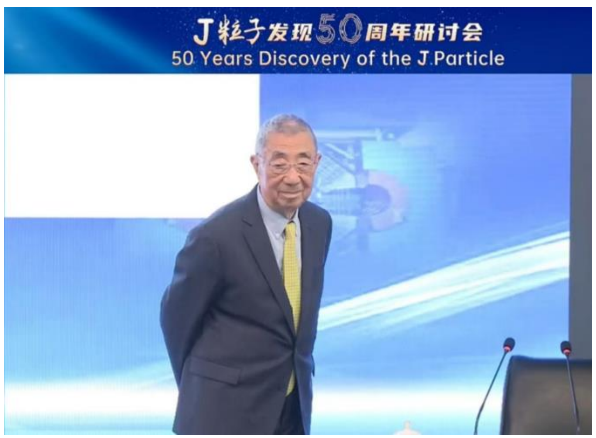

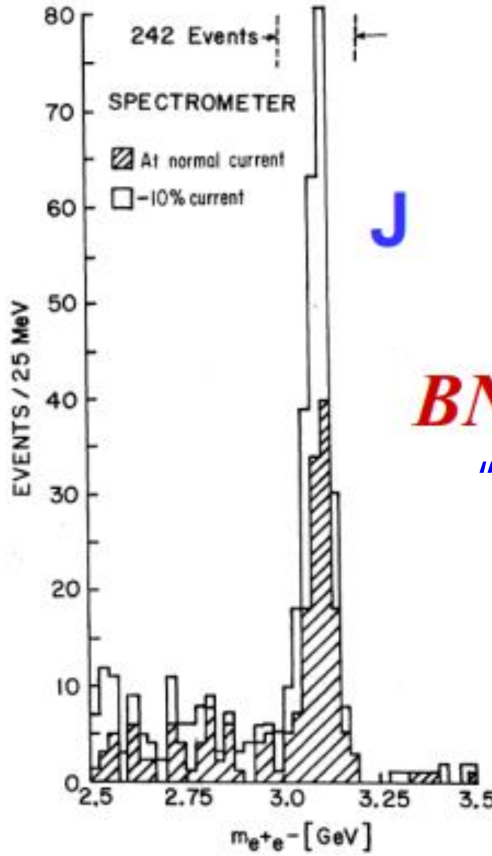

J.J. Aubert et al., PRL 33, 1404 (1974)

J

Discovery of the fourth type of quark:
Charm quark

BNL

"November Revolution in Physics"

Nobel Prize 1976

Scattering experiment must have **particle source**, target material, and detector.

Hyperon source

Baryon octet

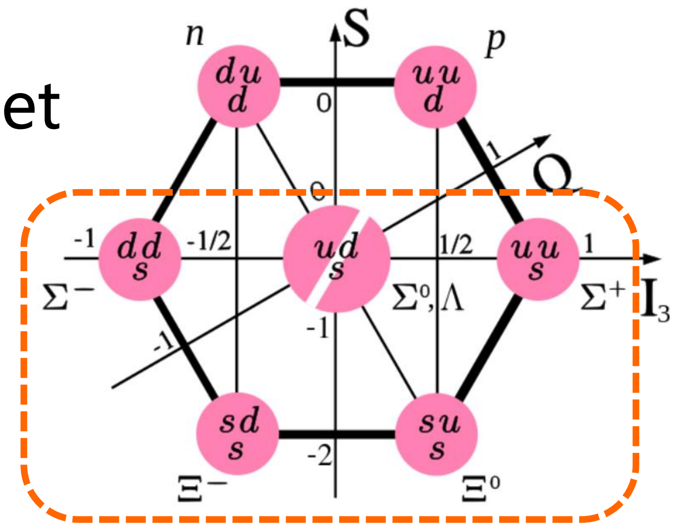

One of main goals of nuclear physics is to understand baryon-baryon interaction in a unified perspective

Limited by availability and short-lifetime of hyperon beams

- Hyperons are obtained by bombarding hydrogen bubble chamber or scintillating fiber target with K^{-}.

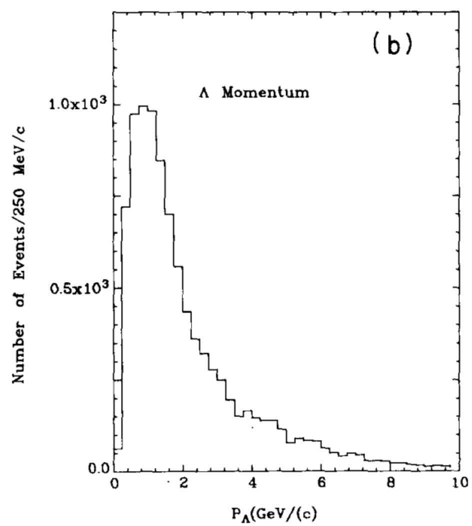

NPB 125, 29 (1977)

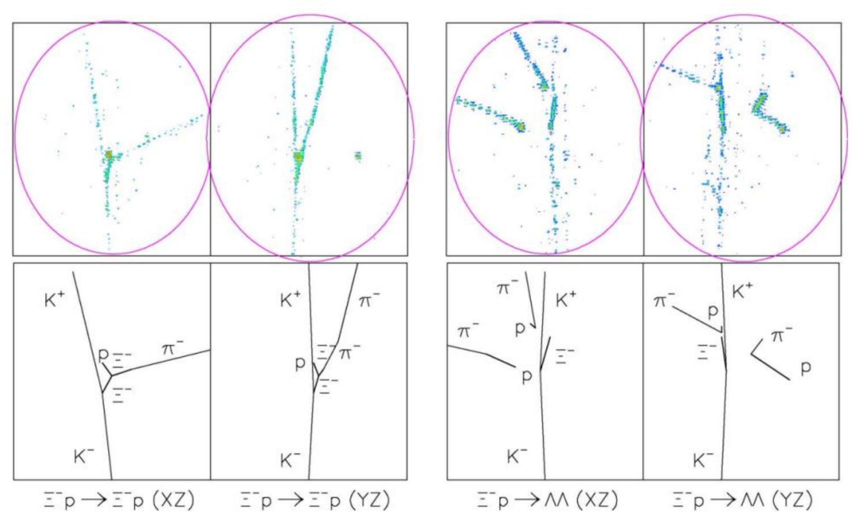

PLB 633, 214 (2006)

Hyperon source

- Hyperons are obtained by bombarding hydrogen bubble chamber or scintillating fiber target with K^-.
- Intensity of hyperon beams is low, experimental measurements are scarce and have large uncertainty.
- No anti-hyperon source.

Reaction	Number of events	
$\Lambda p \to \Lambda p$ (elastic)	584	(1)
$\Lambda p \to \Sigma^- p \pi^+$	132	(2)
$\Lambda p \to \Sigma^+ p \pi^-$	60	(3)
$\Lambda p \to \Lambda p \pi^+ \pi^-$	181	(4)
$\Lambda p \to \Sigma^0 p$	35	(5)
various $\Xi^0 p$ interactions	25	

PLB 32, 720 (1970)

Reaction	Momentum interval (GeV/c)	Number of events	σ (mb)
$\Lambda p \to$ all	$0.5 \to 1.0$		25.8 ± 6.2
	$1.0 \to 1.5$		31.3 ± 6.5
	$1.5 \to 2.0$		42.8 ± 7.1
	$2.0 \to 2.5$		37.5 ± 7.2
	$2.5 \to 3.0$		34.1 ± 8.3
	$3.0 \to 4.0$		41.8 ± 10.0
$\Lambda p \to \Lambda p$	$0.5 \to 1.0$	20	22.2 ± 5.0
	$1.0 \to 1.5$	21	12.9 ± 2.8
	$1.5 \to 2.0$	37	22.0 ± 3.6
	$2.0 \to 2.5$	28	16.1 ± 3.1
	$2.5 \to 3.0$	12	11.0 ± 3.2
	$3.0 \to 4.0$	13	12.5 ± 3.4
$\Lambda p \to \Sigma^0$	$0.66 \to 4.0$	11	1.5 ± 0.5
$\Lambda p \to \Lambda p \pi^0$	$0.88 \to 4.0$	29	4.1 ± 0.8
$\Lambda p \to \Lambda p \pi^+ \pi^-$	$1.36 \to 4.0$	12	1.9 ± 0.6
$\Sigma^+ p \to \Sigma^+ p$	$0.5 \to 1.5$	10	31.2 ± 10.1
	$1.5 \to 2.5$	8	18.7 ± 6.6
	$2.5 \to 4.0$	4	15.3 ± 7.8
$\Sigma^- p \to \Sigma^- p$	$0.5 \to 1.5$	6	13.2 ± 4.7
	$1.5 \to 2.5$	11	13.9 ± 4.1
	$2.5 \to 4.0$	4	7.5 ± 3.8
$\Xi^- p \to \Xi^- p$	$1.0 \to 4.0$	6	13 ± 6
$\Xi^0 p \to \Xi^0 p$	$1.0 \to 4.0$	4	19 ± 10

PLB 38, 123 (1972)

reaction	events *	signature	cross-section events **	cross-section (mb)
$\Xi^0 + p \to \Xi^0 + p$	2	K, Λ	1	8
$\Xi^0 + p \to \Lambda + \Sigma^+$	6	Λ	4	24
$\Xi^0 + p \to \Sigma^0 + \Sigma^+$	1	Λ	1	6
$\Xi^0 + p \to \pi^+ + \Lambda + \Lambda$	1	K, Λ	1	6
$\Xi^0 + p \to \pi^0 + \Lambda + \Sigma^+$	1	Λ	1	6
$\Xi^0 + p \to \pi^+ + \Xi^- + p$	1	K or Λ	1	5
$\Xi^0 + p \to \pi^+ + \pi^+ + \Xi^- + n$	1	K, Λ	1	6
$\Xi^0 + p \to \Xi^- + p$	2	Λ	2	8
$\Xi^0 + p \to \Sigma^- + \Sigma^+$	1	K	1	4
$\Xi^0 + p \to \Sigma^- + K^0 + p$	1	K	1	4

NPB 125, 29 (1977)

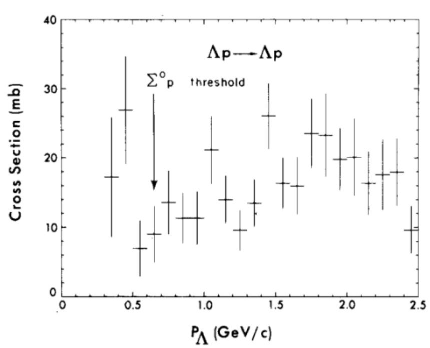

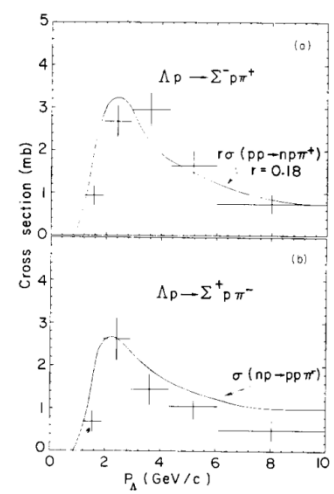

PLB 633, 214 (2006)

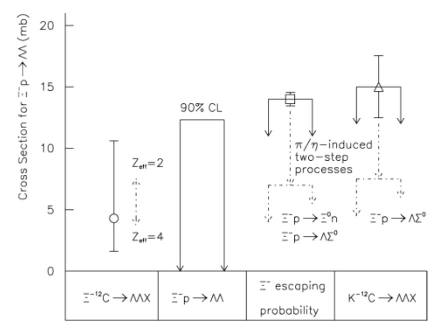

Theory of hyperon-nucleon (YN) interaction has large uncertainty due to lack of relevant measurements

PRC 105, 035203 (2022)

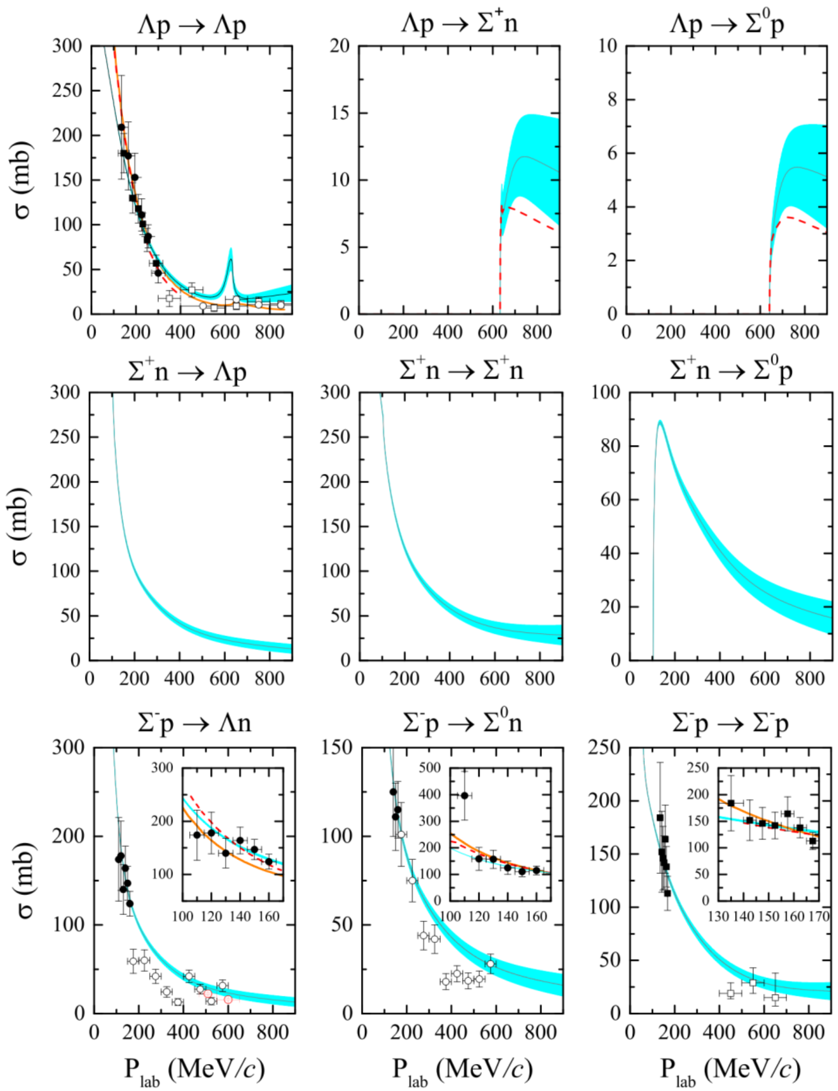

LO : H. Polinder, J.H., U.-G. Meißner, PLB 653 (2007) 29

NLO16: J.H., U.-G. Meißner, S. Petschauer, NPA 954 (2016) 273

NLO19: J.H., U.-G. Meißner, EPJA 55 (2019) 23

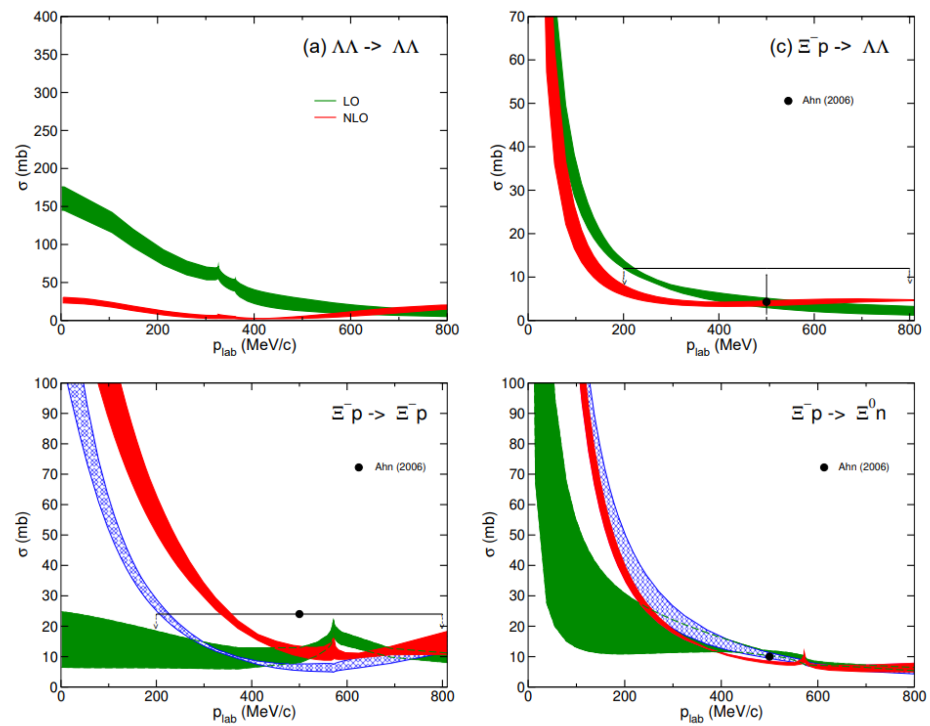

"Hyperon puzzle" of neutron stars

- Hyperons are believed to be appeared in inner core of neutron stars.

$$B_1 \to B_2 + l + \bar{\nu}_l,\ B_2 + l \to B_1 + \nu_l$$

$$n \to p + e^- + \bar{\nu}_e, p + e^- \to n + \nu_e \qquad \Sigma^- \to n + e^- + \bar{\nu}_e, n + e^- \to \Sigma^- + \nu_e$$

$$\Lambda \to p + e^- + \bar{\nu}_e, p + e^- \to \Lambda + \nu_e \qquad \Xi^- \to \Lambda + e^- + \bar{\nu}_e, \Lambda + e^- \to \Xi^- + \nu_e$$

- Appearance of hyperons softens equation of state, lead to maximum mass that neutron stars can sustain is less than mass of already-observed neutron stars.

- A repulsive force is introduced to stiffen equation of state in theory, such as a combination of ΛN and ΛNN interactions. Study of hyperon-nucleon interaction is crucial to solve "hyperon puzzle" of neutron stars.

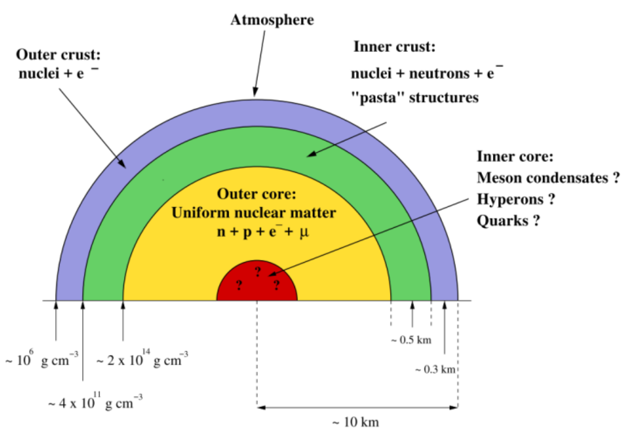

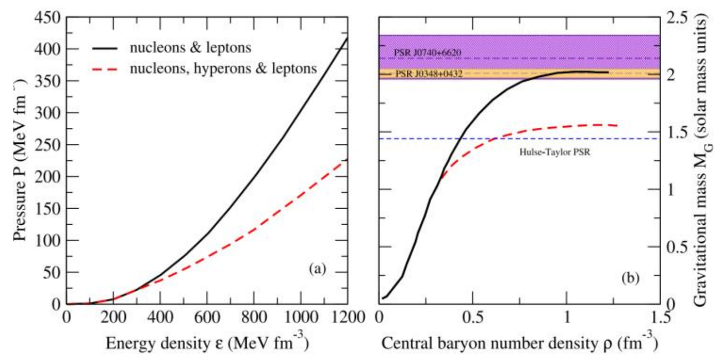

PPNP 112, 103770 (2020)

PRL 114, 092301 (2015)

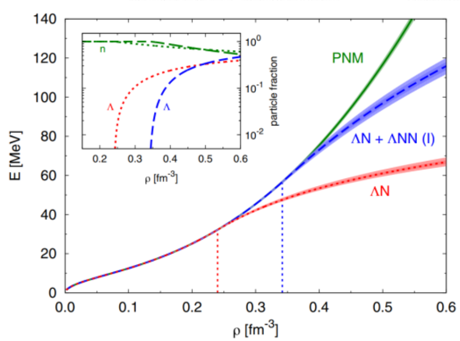

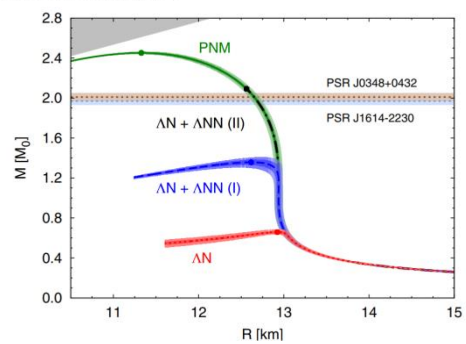

Search for H-dibaryon

- Study of hyperon-nucleon interaction can be used to search for the H-dibaryon, which has strangeness -2 and valence quark structure $uuddss$. This H-dibaryon is firstly predicted according to the bag model as early as the 1970s. Later, two lattice QCD groups also study this respectively, and both predict the existence of H-dibaryon.
- However, so far, although the H-dibaryon has been searched by many experiments, no any convincing signals has been found.
- H-dibaryon can be searched in the final states of reaction process of Ξ and nucleon. And H-dibaryon is also predicted to appear as a bound state of $\Sigma\Sigma$ decaying strongly into ΞN or $\Lambda\Lambda$.

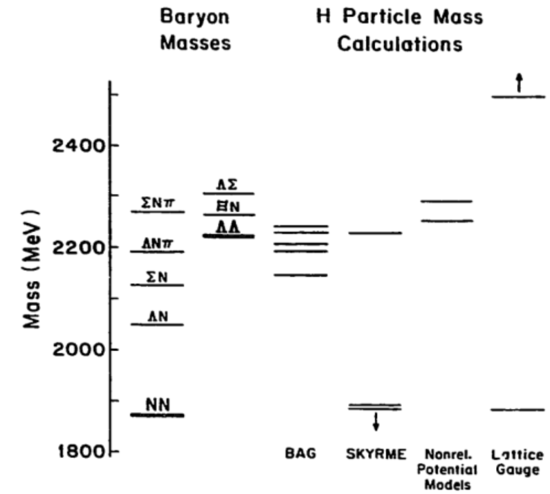

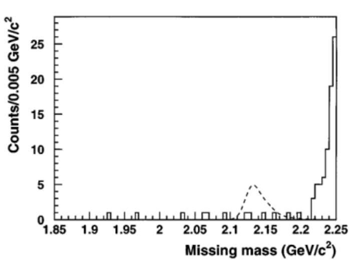

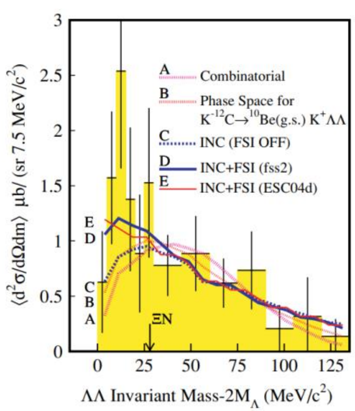

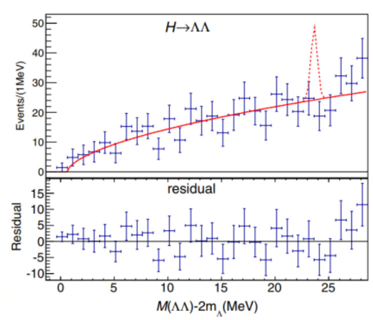

R. L. Jaffe, Phys. Rev. Lett. **38**, 195 (1977).

A. T. M. Aerts, P. J. G. Mulders and J. J. de Swart, Phys. Rev. D **17**, 260 (1978).

T. Inoue *et al.* [HAL QCD], Phys. Rev. Lett. **106**, 162002 (2011).

S. R. Beane *et al.* [NPLQCD], Phys. Rev. Lett. **106**, 162001 (2011).

S. R. Beane *et al.* [NPLQCD], Mod. Phys. Lett. A **26**, 2587 (2011).

D. P. Goyal, J. N. Misra and A. V. Sodhi, Phys. Rev. D **21**, 607 (1980).

S. Paul, Nucl. Phys. B Proc. Suppl. **21**, 243 (1991).

J. Belz *et al.*, Phys. Rev. Lett. **76**, 3277 (1996).

R. W. Stotzer *et al.* [BNL E836 Collaboration], Phys. Rev. Lett. **78**, 3646 (1997).

J. K. Ahn *et al.* [KEK-PS E224 Collaboration], Phys. Lett. B **444**, 267 (1998).

A. Alavi-Harati *et al.* [KTeV Collaboration], Phys. Rev. Lett. **84**, 2593 (2000).

C. J. Yoon *et al.* [KEK-PS E522 Collaboration], Phys. Rev. C **75**, 022201 (2007).

B. H. Kim *et al.* [Belle Collaboration], Phys. Rev. Lett. **110**, 222002 (2013).

Some recent experimental results on hyperon-nucleon scattering

PHYSICAL REVIEW LETTERS **127**, 272303 (2021)

(CLAS Collaboration)

Improved Λp Elastic Scattering Cross Sections between 0.9 and 2.0 GeV/c as a Main Ingredient of the Neutron Star Equation of State

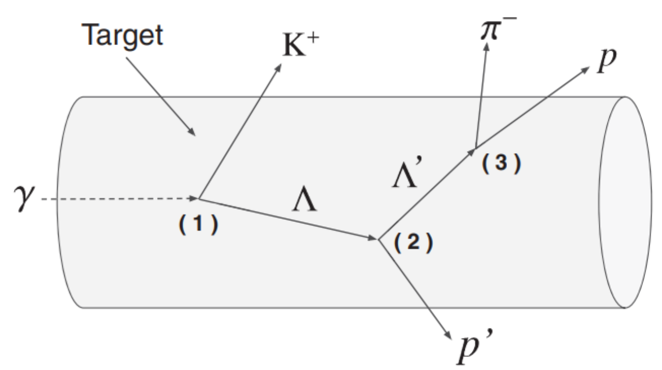

$$\sigma(p_\Lambda) = \frac{Y(p_\Lambda)}{A(p_\Lambda) \times \mathcal{L}(p_\Lambda) \times \Gamma}$$

$$\mathcal{L}(p_\Lambda) = \frac{N_A \times \rho_T \times l}{M} N_\Lambda(p_\Lambda)$$

$\Lambda p \to \Lambda p$

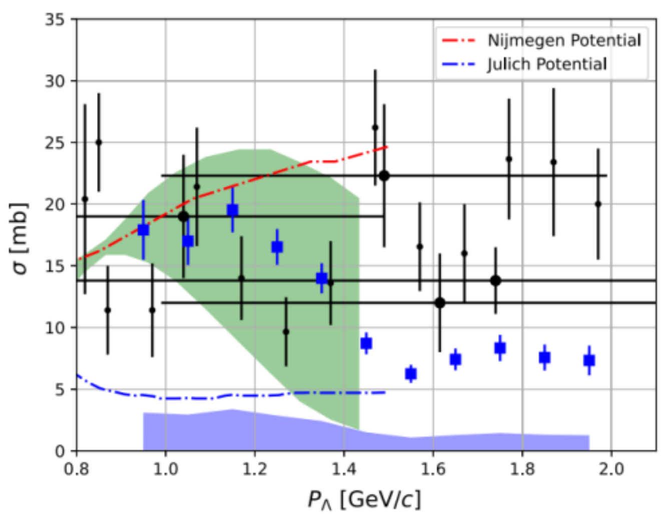

This is the first data on this reaction since the 1970s.

Some recent experimental results on hyperon-nucleon scattering

J-PARC E40 Collaboration

PRC 104, 045204 (2021)

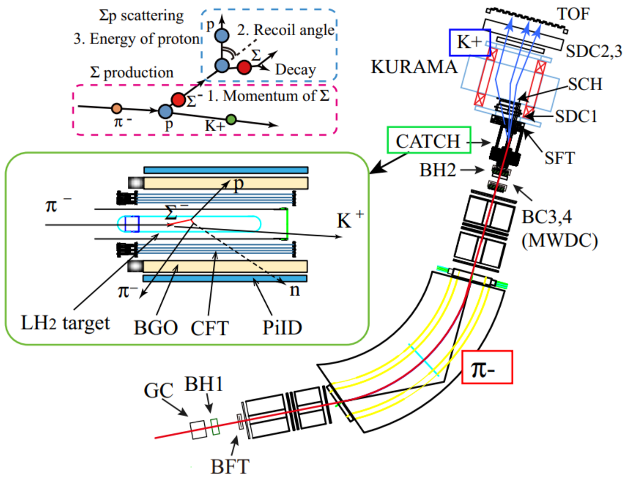

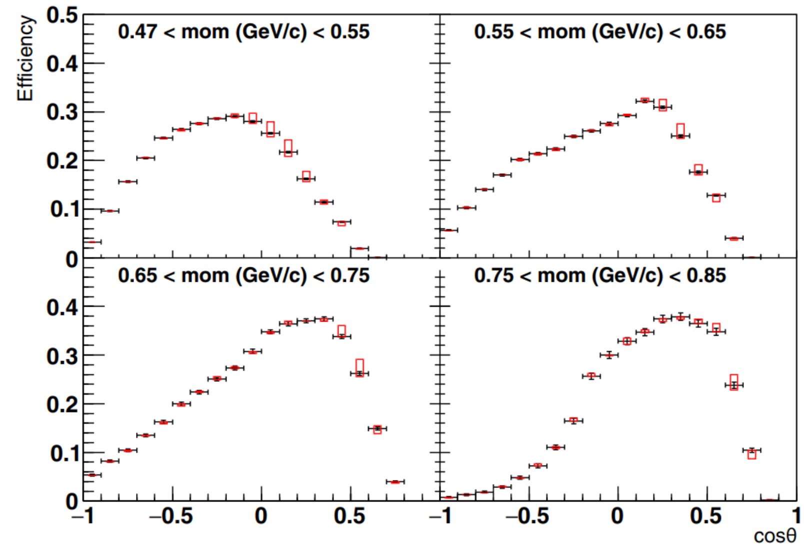

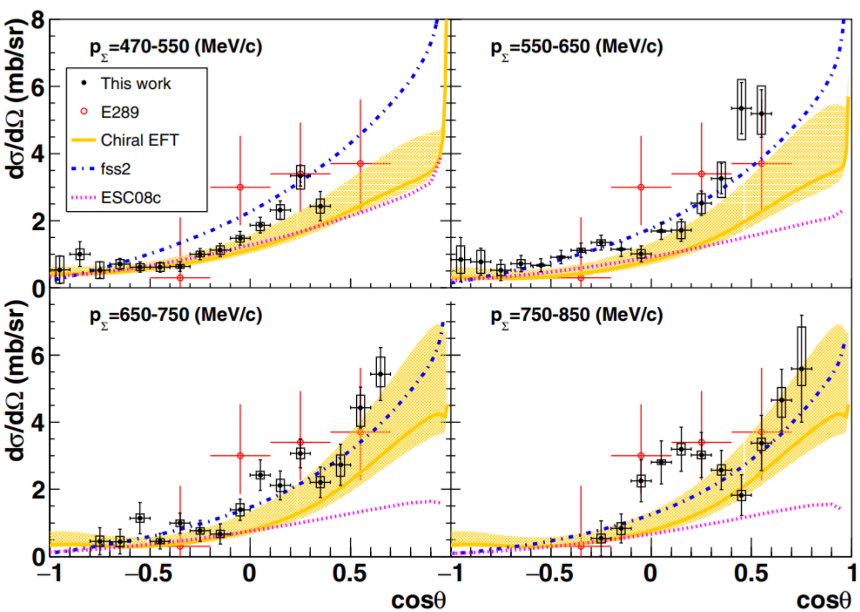

$$\Sigma^- p \rightarrow \Sigma^- p$$

Some recent experimental results on hyperon-nucleon scattering

J-PARC E40 Collaboration

PTEP 2022, 093D01 (2022)

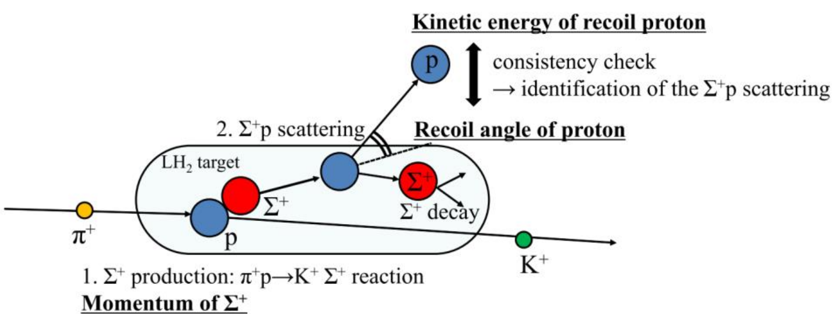

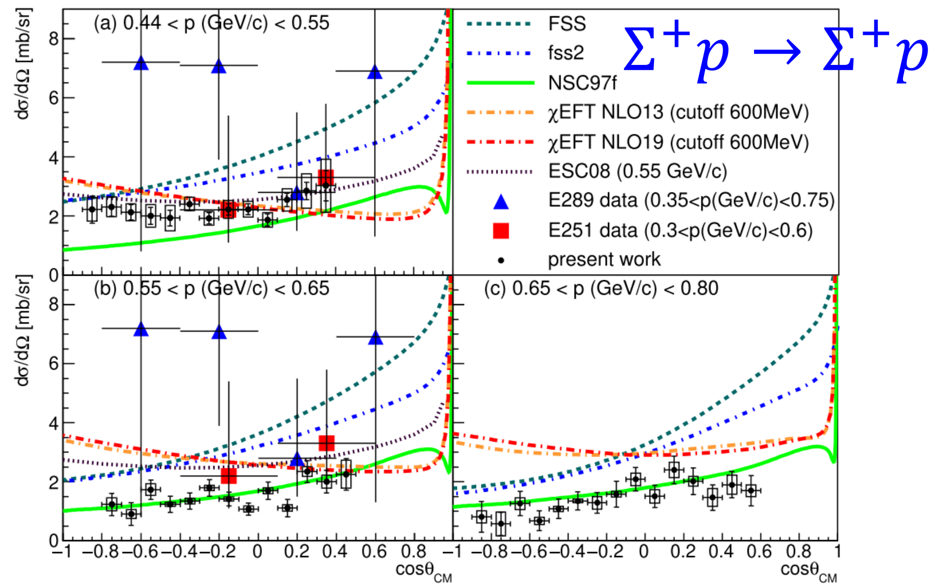

PRL 128, 072501 (2022)

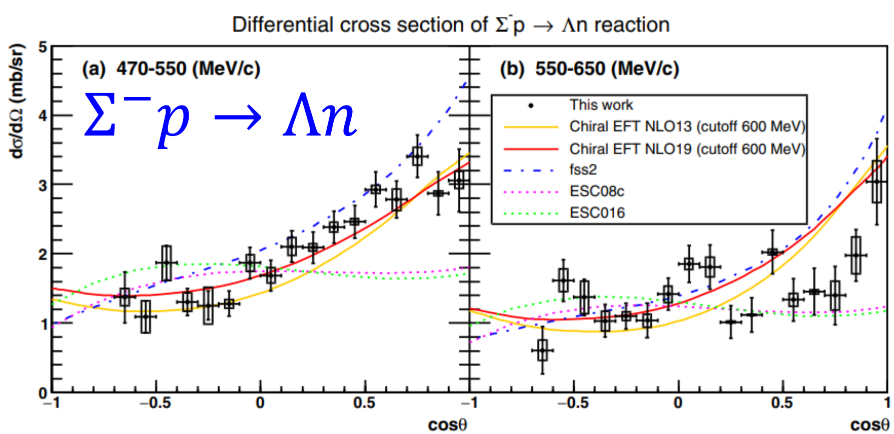

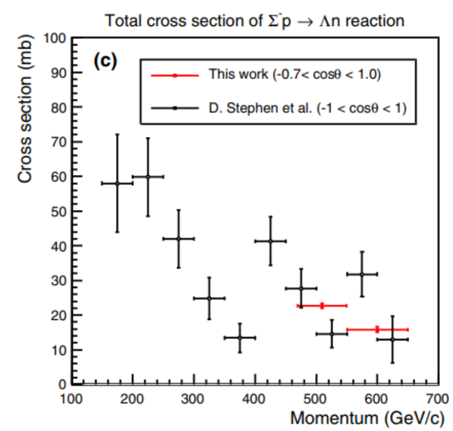

Beijing Electron Positron Collider II (BEPCII) and Beijing Spectrometer III (BESIII)

tau-charm energy region

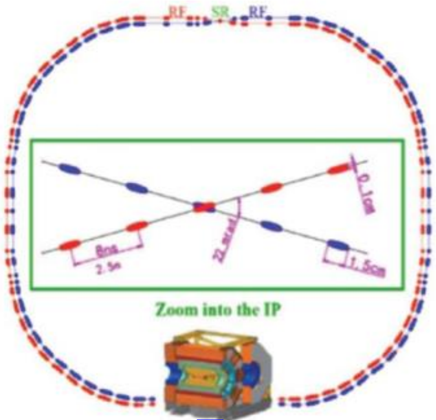

Storage ring

Linear accelerator

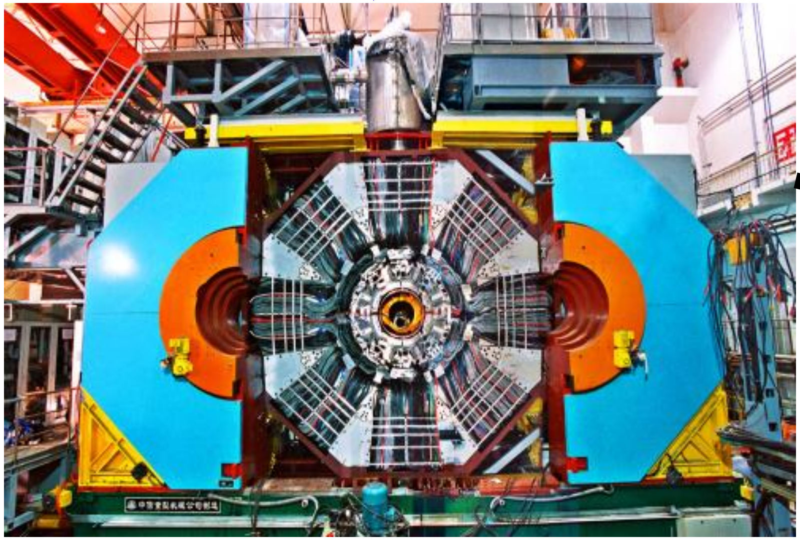

BESIII detector

BEPCII

BESIII detector

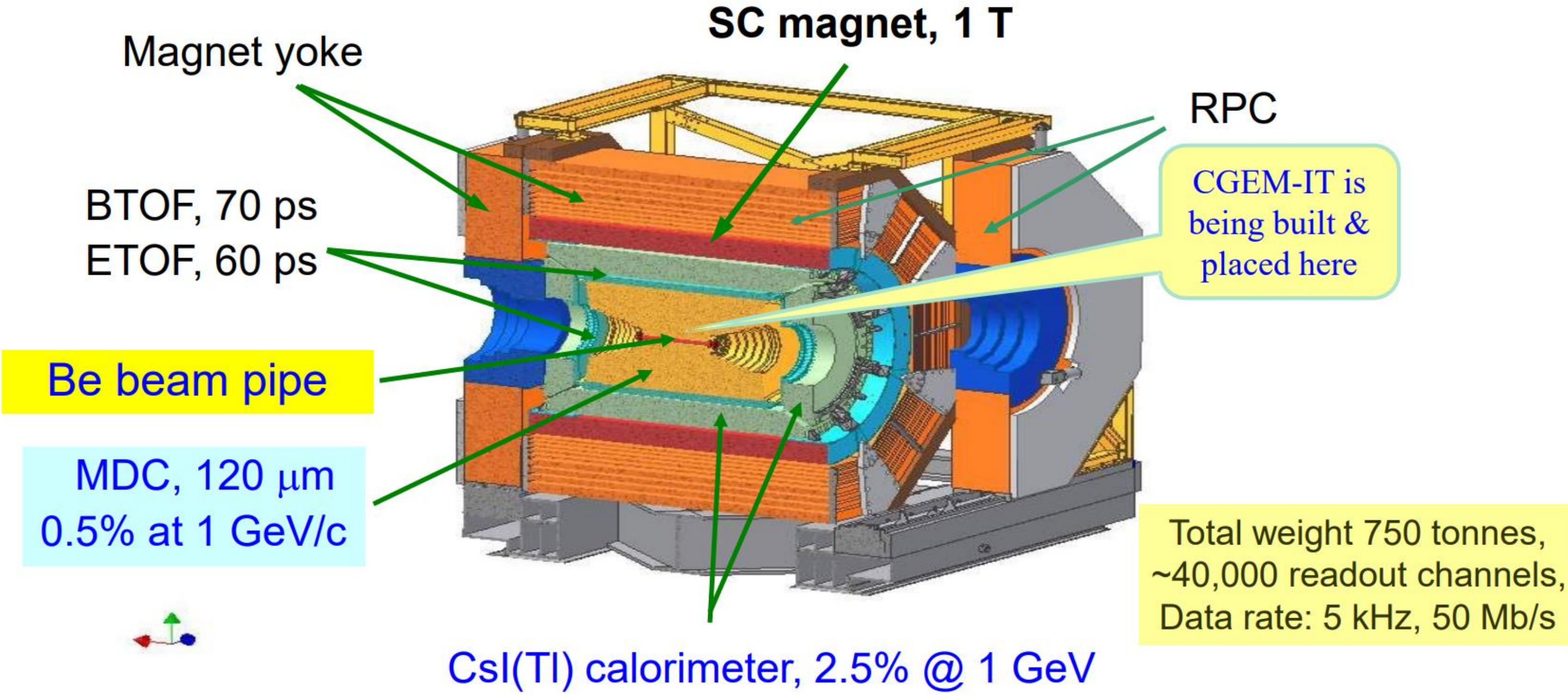

Has been in full operation since 2008,
all subdetectors are in very good status!

BESIII data samples

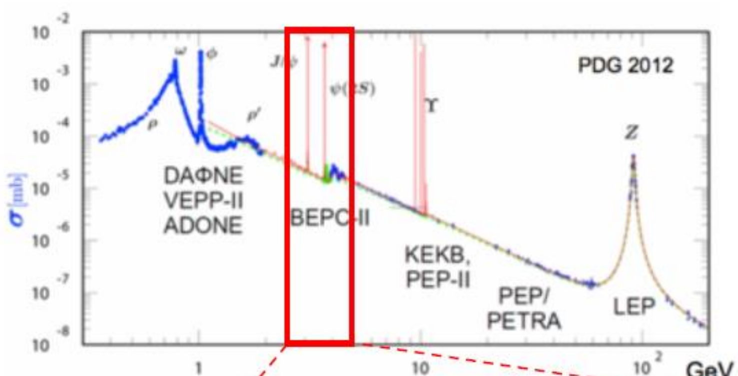

BESIII has collected the largest data samples of the J/ψ and $\psi(3686)$ in the world, and $> 20\ \mathrm{fb}^{-1}$ above $4.0\ \mathrm{GeV}$ in total.

10 billion J/ψ events

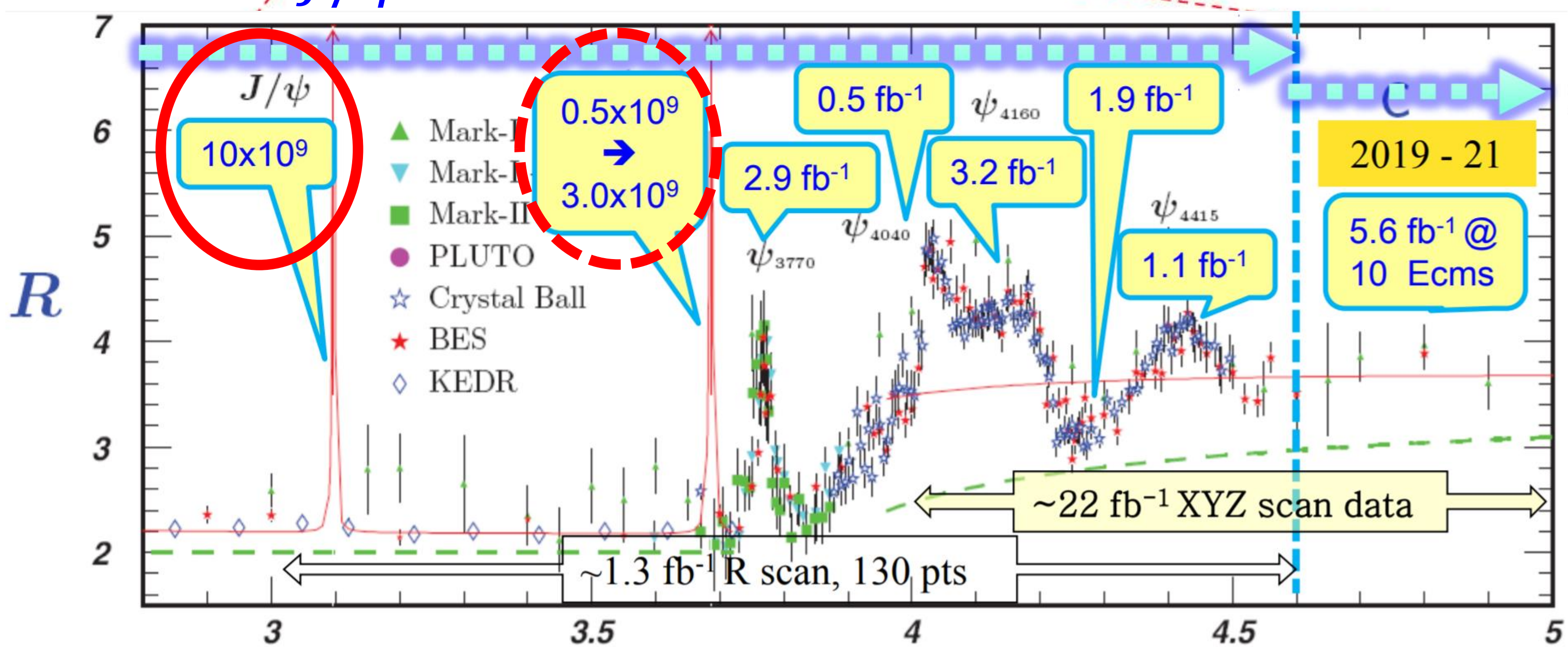

Experimental study on particle targeting at BESIII

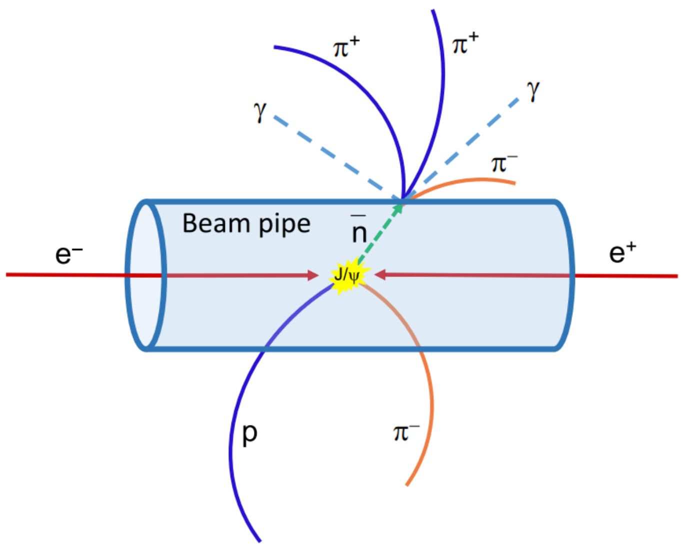

PRL 127, 012003 (2021)
CPC 48, 073003 (2024)

$\bar{n}p \rightarrow \pi^+\pi^+\pi^-\pi^0, \pi^0 \rightarrow \gamma\gamma$

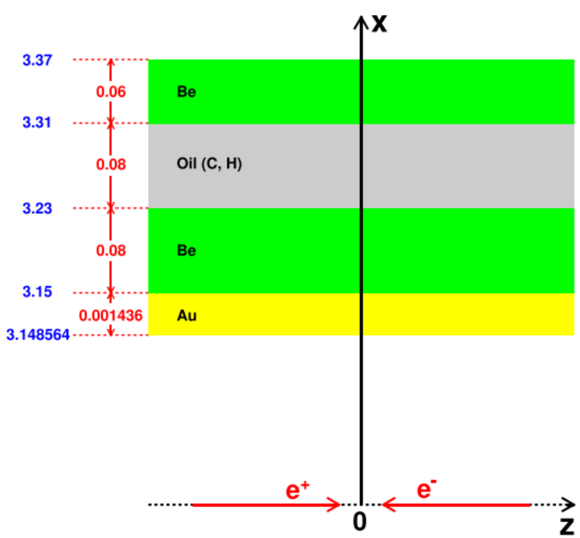

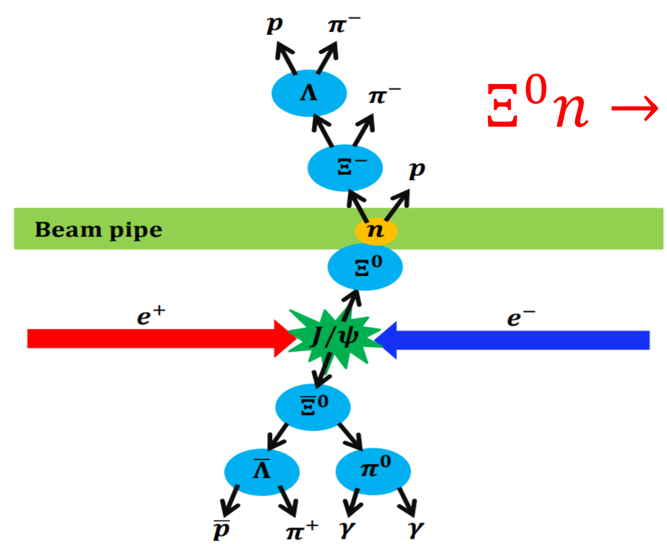

$\Xi^0 n \rightarrow \Xi^- p$

particle source: hyperon from J/ψ decays
target material: beam pipe
detector: BESIII detector

Experimental study on particle targeting at BESIII

Hyperon/Antihyperon	τ ($\times 10^{-10}$s)	Decay mode	$\mathcal{B}$ ($\times 10^{-3}$)	P (GeV/c)	$E_{\rm cm}$ (GeV)	N ($\times 10^5$)	$N^{\rm bp}$ ($\times 10^5$)
$\Lambda/\bar{\Lambda}$	2.62	$J/\psi \to \Lambda\bar{\Lambda}$	1.88	1.074	2.24	188	102
$\Sigma^+/\bar{\Sigma}^-$	0.80	$J/\psi \to \Sigma^+\bar{\Sigma}^-$	1.07	0.992	2.28	107	15
$\Xi^0/\bar{\Xi}^0$	2.90	$J/\psi \to \Xi^0\bar{\Xi}^0$	1.17	0.818	2.35	117	51
$\Xi^-/\bar{\Xi}^+$	1.64	$J/\psi \to \Xi^-\bar{\Xi}^+$	0.97	0.807	2.35	97	23
$\Lambda/\bar{\Lambda}$	2.62	$\psi(2S) \to \Lambda\bar{\Lambda}$	0.38	1.467	2.36	11	7
$\Sigma^+/\bar{\Sigma}^-$	0.80	$\psi(2S) \to \Sigma^+\bar{\Sigma}^-$	0.24	1.408	2.40	7	2
$\Xi^0/\bar{\Xi}^0$	2.90	$\psi(2S) \to \Xi^0\bar{\Xi}^0$	0.23	1.291	2.47	7	4
$\Xi^-/\bar{\Xi}^+$	1.64	$\psi(2S) \to \Xi^-\bar{\Xi}^+$	0.29	1.284	2.47	9	3
$\Omega^-/\bar{\Omega}^+$	0.82	$\psi(2S) \to \Omega^-\bar{\Omega}^+$	0.06	0.774	2.67	2	0.1

The abundant hyperon-antihyperon pairs are produced, also as antihyperon sources.

Recent results on hyperon-nucleon interactions at BESIII

- **First Study of Reaction $\Xi^0 n \to \Xi^- p$ Using Ξ^0-Nucleus Scattering at an Electron-Positron Collider**
  PRL 130, 251902 (2023)

- **First measurement of ΛN inelastic scattering with Λ from $e^+e^- \to J/\psi \to \Lambda\bar{\Lambda}$**
  PRC 109, L052201 (2024)

- **First Study of Antihyperon-Nucleon Scattering $\bar{\Lambda}p \to \bar{\Lambda}p$ and Measurement of $\Lambda p \to \Lambda p$ Cross Section**
  PRL 132, 231902 (2024)

Study of $\Xi^0 n \to \Xi^- p$

PRL 130, 251902 (2023)

Reaction chain :

$J/\psi \to \Xi^0\bar{\Xi}^0$, $\bar{\Xi}^0 \to \bar{\Lambda}\pi^0$, $\bar{\Lambda} \to \bar{p}\pi^+$, $\pi^0 \to \gamma\gamma$,
$\Xi^0 n \to \Xi^- p$, $\Xi^- \to \Lambda\pi^-$, $\Lambda \to p\pi^-$.

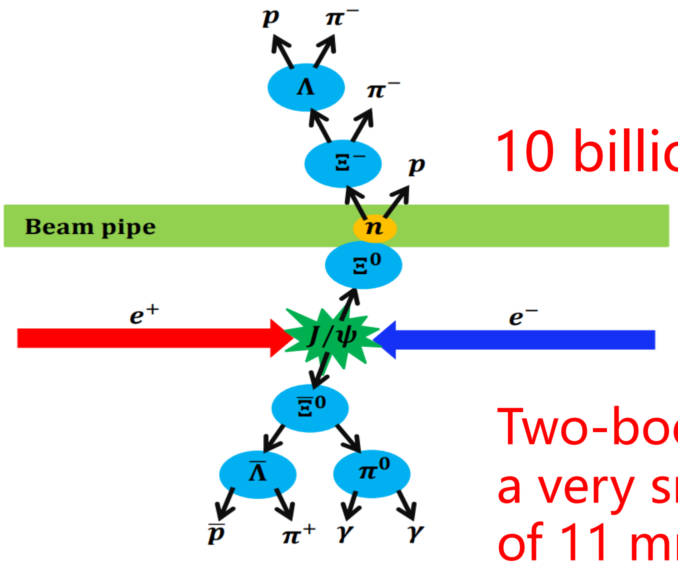

10 billion J/ψ data

Two-body decay, $P_{\Xi^0} \approx 0.818\ \mathrm{GeV}/c$, a very small horizontal crossing angle of 11 mrad for e^+ and e^- beams.

Analysis method :

Using $\bar{\Xi}^0$ to tag the event and requiring the recoiling mass in Ξ^0 region. Then reconstructing Ξ^- and p in the signal side.

Study of $\Xi^0 n \to \Xi^- p$

R_{xy} is distance from reconstructed $\Xi^- p$ vertex to z axis

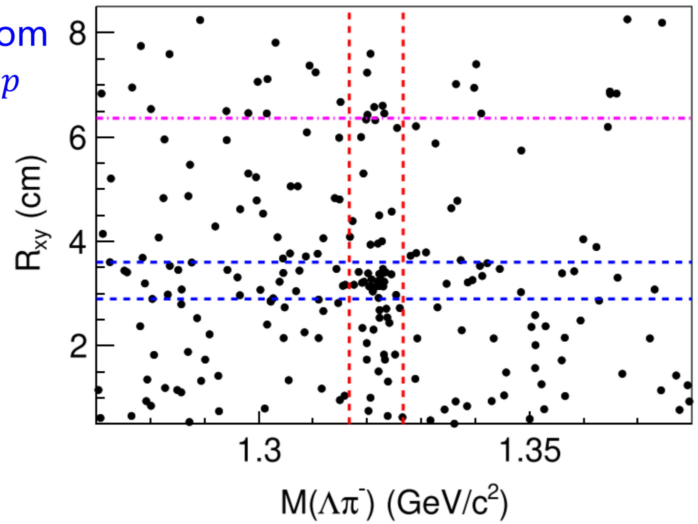

Inner wall of MDC

Beam pipe

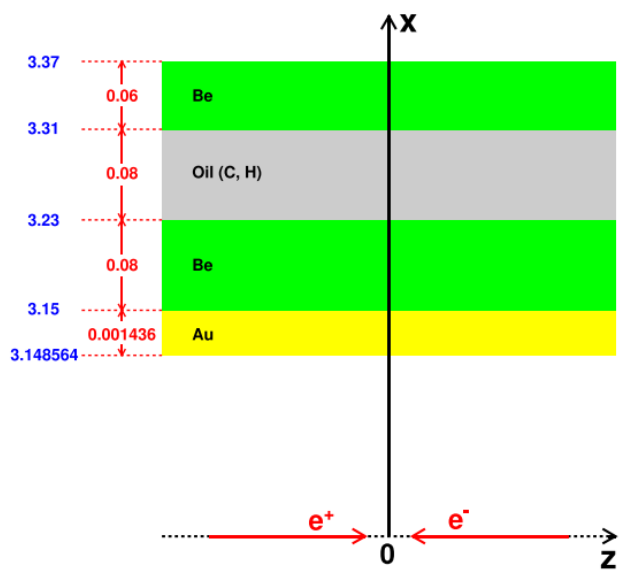

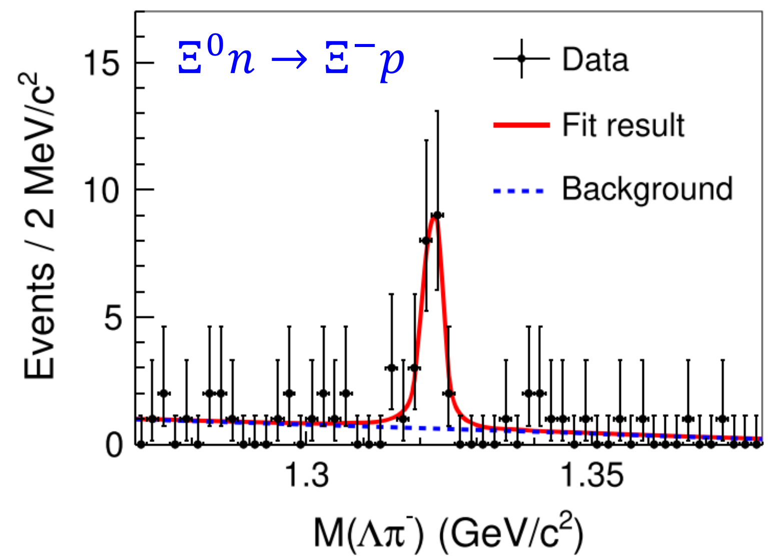

$N = 22.9 \pm 5.5$

$S = 7.1\sigma$

Cross section of $\Xi^0 + {}^9\mathrm{Be} \to \Xi^- + p + {}^8\mathrm{Be}$

$$\sigma(\Xi^0 + {}^9\mathrm{Be} \to \Xi^- + p + {}^8\mathrm{Be}) = \frac{N^{\mathrm{sig}}}{\epsilon \mathcal{B} \mathcal{L}_{\mathrm{eff}}}$$

$$\mathcal{L}_{\mathrm{eff}} = \frac{N_{J/\psi}\mathcal{B}_{J/\psi}}{2+\frac{2}{3}\alpha}\int_a^b \int_0^\pi (1+\alpha\cos^2\theta)e^{-\frac{x}{\sin\theta\beta\gamma L}} N(x)C(x)\,d\theta\,dx$$

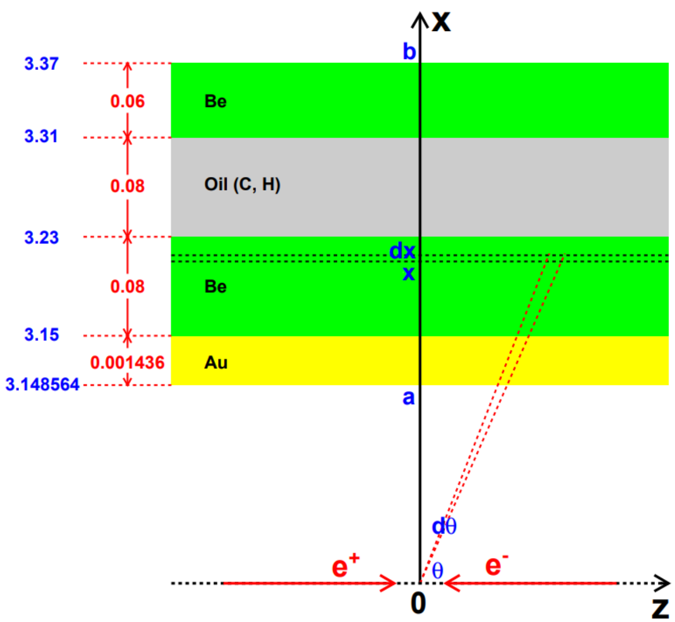

Parameter	Result
N^{sig}	22.9 ± 5.5
ϵ	1.873%
$\mathcal{B}$	$(40.114 \pm 0.444)\%$ [53]
$N_{J/\psi}$	$(1.0087 \pm 0.0044) \times 10^{10}$ [46]
$\mathcal{B}_{J/\psi}$	$(0.117 \pm 0.004)\%$ [53]
α	0.514 ± 0.016 [56]
L	(8.69 ± 0.27) cm [53]
E_{beam}	1.5485 GeV
m_{Ξ^0}	$(1.31486 \pm 0.00020)\ \mathrm{GeV}/c^2$ [53]
a	3.148564 cm [45]
b	3.37 cm [45]
$N(x)$	$\begin{cases} 5.91 \times 10^{22}\ \mathrm{cm}^{-3}, & 3.148564 \le x \le 3.15\ \mathrm{cm} \\ 1.24 \times 10^{23}\ \mathrm{cm}^{-3}, & 3.15 < x \le 3.23\ \mathrm{cm} \\ 3.45 \times 10^{22}\ \mathrm{cm}^{-3}, & 3.23 < x \le 3.31\ \mathrm{cm} \\ 1.24 \times 10^{23}\ \mathrm{cm}^{-3}, & 3.31 < x \le 3.37\ \mathrm{cm} \end{cases}$
$C(x)$	$\begin{cases} 8.437(23.6), & 3.148564 \le x \le 3.15\ \mathrm{cm} \\ 1.000(1.00), & 3.15 < x \le 3.23\ \mathrm{cm} \\ 1.090(1.20), & 3.23 < x \le 3.31\ \mathrm{cm} \\ 1.000(1.00), & 3.31 < x \le 3.37\ \mathrm{cm} \end{cases}$

$\sigma \propto A^{\alpha'}$

α' is about $\frac{2}{3} \sim 1$

pure surface process assumption
(proportional to number of neutrons)

Study of $\Xi^0 n \to \Xi^- p$

The measured cross section of the reaction process $\Xi^0 + {}^9\mathrm{Be} \to \Xi^- + p + {}^8\mathrm{Be}$ is $\sigma(\Xi^0 + {}^9\mathrm{Be} \to \Xi^- + p + {}^8\mathrm{Be}) = (22.1 \pm 5.3_{\mathrm{stat}} \pm 4.5_{\mathrm{sys}})$ mb at $P_{\Xi^0} \approx 0.818\ \mathrm{GeV}/c$.

If we take the effective number of reaction neutrons in ${}^9\mathrm{Be}$ nucleus as 3, the cross section of $\Xi^0 n \to \Xi^- p$ for single neutron is determined to be $\sigma(\Xi^0 n \to \Xi^- p) = (7.4 \pm 1.8_{\mathrm{stat}} \pm 1.5_{\mathrm{sys}})$ mb, consistent with theoretical predictions.

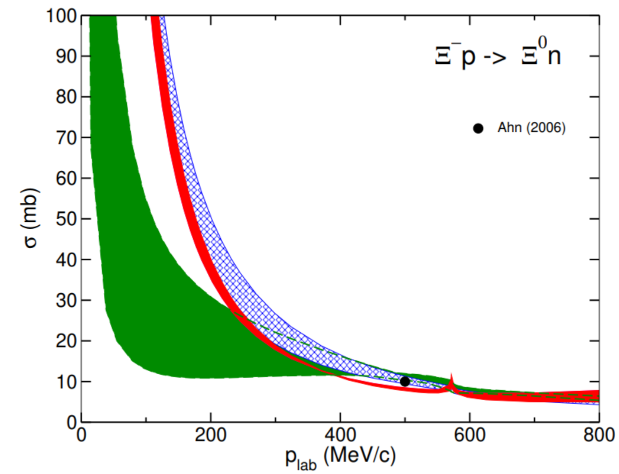

LO : H. Polinder, J.H., U.-G. Meißner, PLB 653 (2007) 29
NLO16: J.H., U.-G. Meißner, S. Petschauer, NPA 954 (2016) 273
NLO19: J.H., U.-G. Meißner, EPJA 55 (2019) 23

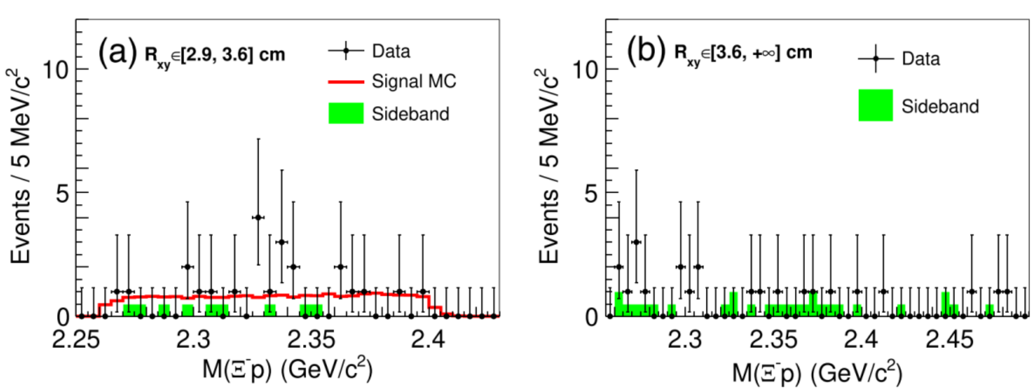

No significant H-dibaryon signals are seen

This work is the first study of hyperon-nucleon interaction in electron-positron collisions, and opens up a new direction for such research.

Study of $\Lambda N \to \Sigma^+ X$

PRC 109, L052201 (2024)

Reaction chain :

$J/\psi \to \Lambda\bar{\Lambda}$, $\bar{\Lambda} \to \bar{p}\pi^+$, $\Lambda + N(\text{nucleus}) \to \Sigma^+ + X(\text{anything})$, $\Sigma^+ \to p\pi^0$, $\pi^0 \to \gamma\gamma$.

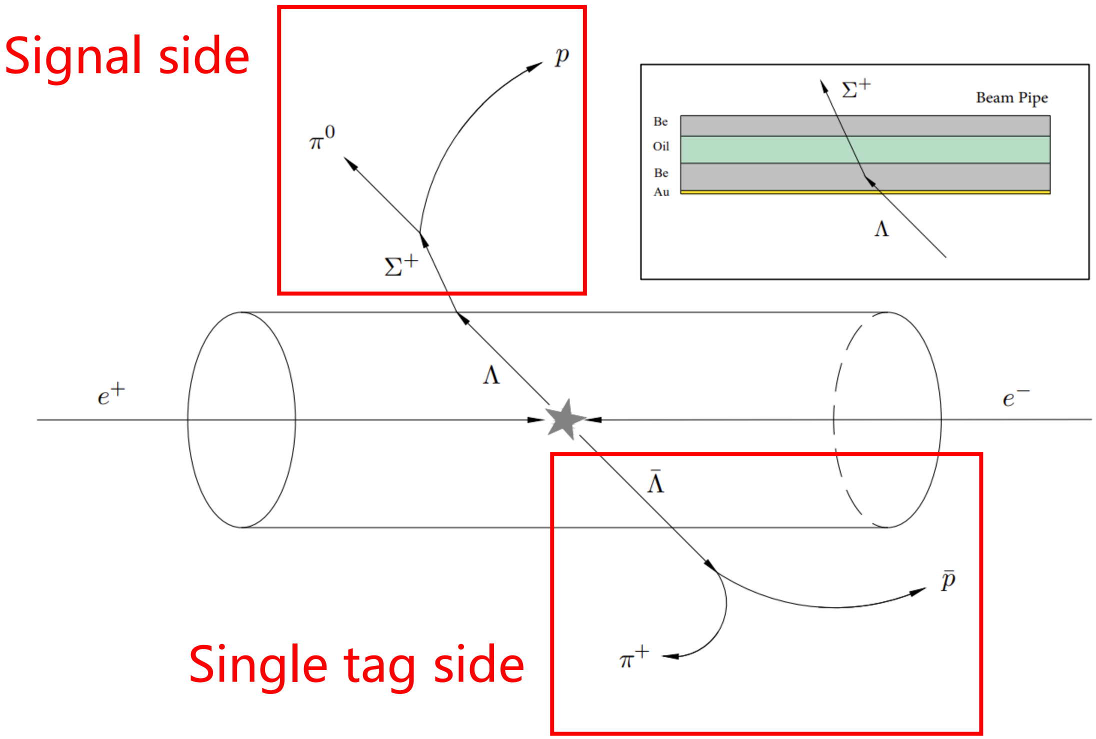

Two-body decay, $P_\Lambda \approx 1.074\ \mathrm{GeV}/c$,

a very small horizontal crossing angle of 11 mrad for e^+ and e^- beams, resulting in a small range of $0.017\ \mathrm{GeV}/c$ above and below $1.074\ \mathrm{GeV}/c$ for P_Λ.

Study of $\Lambda N \to \Sigma^+ X$

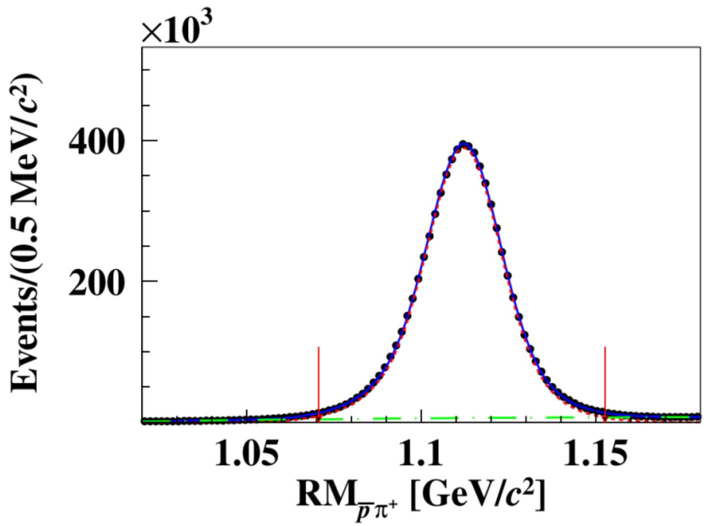

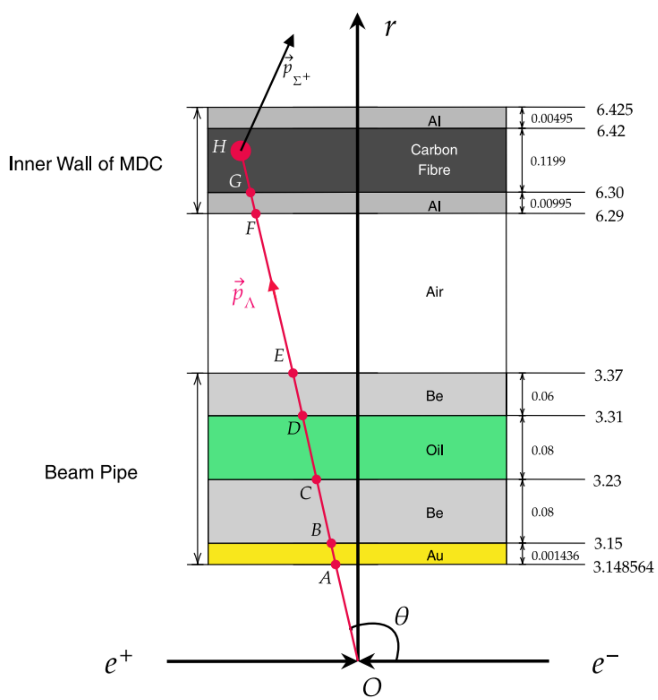

$N_{\mathrm{ST}} = 7207565 \pm 3741$

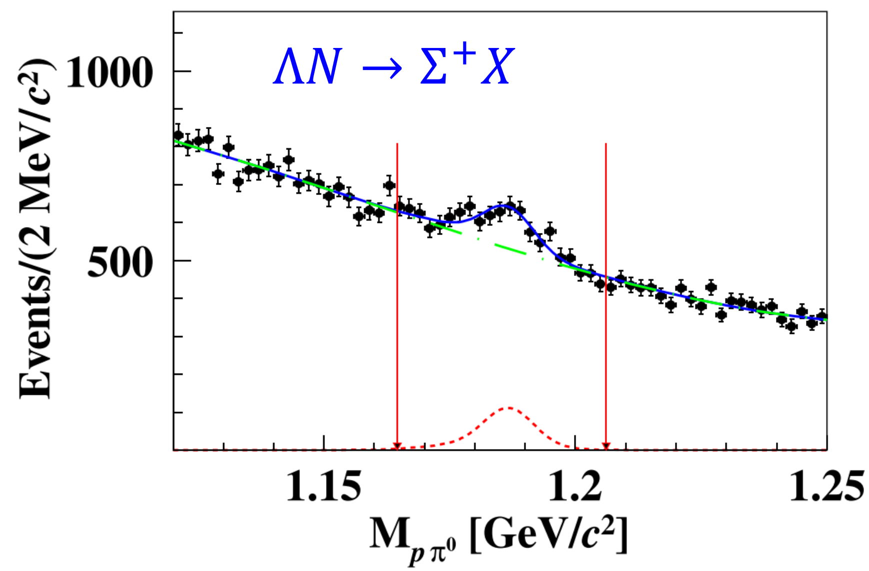

$N_{\mathrm{DT}} = 795 \pm 101$

The reaction position can not be determined. These signal events mainly come from the reaction with beam pipe and inner wall of MDC.

Cross section of $\Lambda + {}^9\mathrm{Be} \to \Sigma^+ + X$

$$\sigma(\Lambda + {}^9\mathrm{Be} \to \Sigma^+ + X) = \frac{N_{\mathrm{DT}}}{\epsilon_{\mathrm{sig}} \mathcal{L}_\Lambda} \frac{1}{\mathcal{B}(\Sigma^+ \to p\pi^0)}$$

$$\mathcal{L}_\Lambda = N_{\mathrm{ST}} \frac{N_A}{N_{\mathrm{ST}}^{\mathrm{MC}}} \sum_j^7 \sum_i^{N_{\mathrm{ST}}^{\mathrm{MC}}} \frac{\rho_T^j l^{ij}}{M^j} \mathcal{R}_\sigma^j$$

path length of incident Λ of i_{th} event inside j_{th} layer

pure surface process assumption (proportional to number of protons)

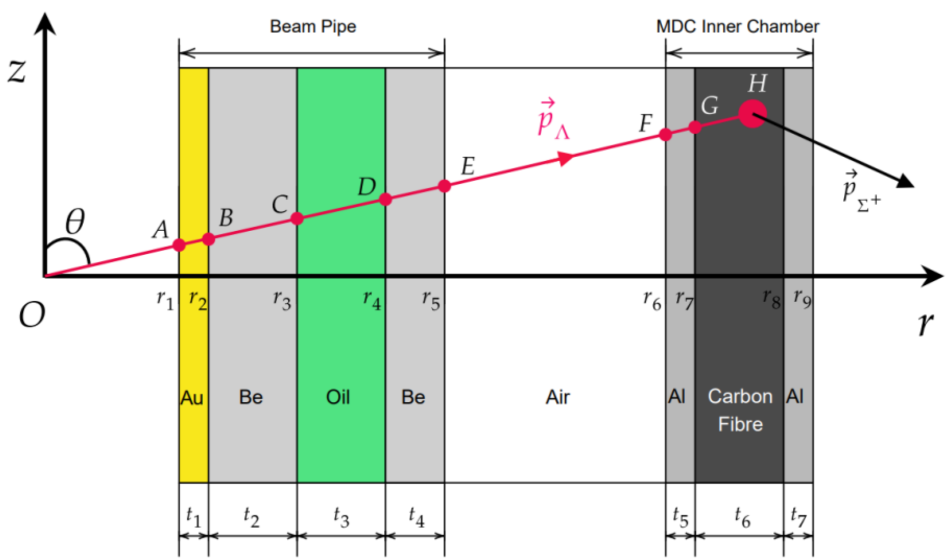

Parameter	Value
N_{DT}	795 ± 101
ϵ_{sig}	24.32%
$\mathcal{L}_\Lambda$	$(17.00 \pm 0.01) \times 10^{28}\ \mathrm{cm}^{-2}$
$\mathcal{B}(\Sigma^+ \to p\pi^0)$	$(51.57 \pm 0.30)\%$

Study of $\Lambda N \to \Sigma^+ X$

The measured cross section of the reaction process $\Lambda + {}^9\mathrm{Be} \to \Sigma^+ + X$ is $\sigma(\Lambda + {}^9\mathrm{Be} \to \Sigma^+ + X) = (37.3 \pm 4.7_{\mathrm{stat}} \pm 3.5_{\mathrm{sys}})$ mb at $P_\Lambda \approx 1.074$ GeV/c. This work represents the first attempt to investigate Λ-nucleus interaction at an e^+e^- collider.

If taking the effective number of reaction protons in ${}^9\mathrm{Be}$ nucleus as 1.93, the cross section of $\Lambda p \to \Sigma^+ X$ for single proton is determined to be $\sigma(\Lambda p \to \Sigma^+ X) = (19.3 \pm 2.4_{\mathrm{stat}} \pm 1.8_{\mathrm{sys}})$ mb.

$\sigma(\Lambda p \to \Sigma^+ n)$ is twice of $\sigma(\Lambda p \to \Sigma^0 p)$

NPB 125, 29 (1977)

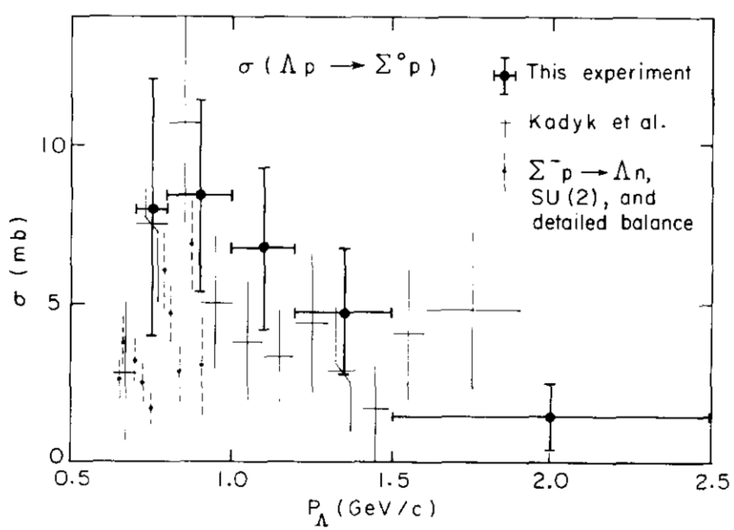

PRC 105, 035203 (2022)

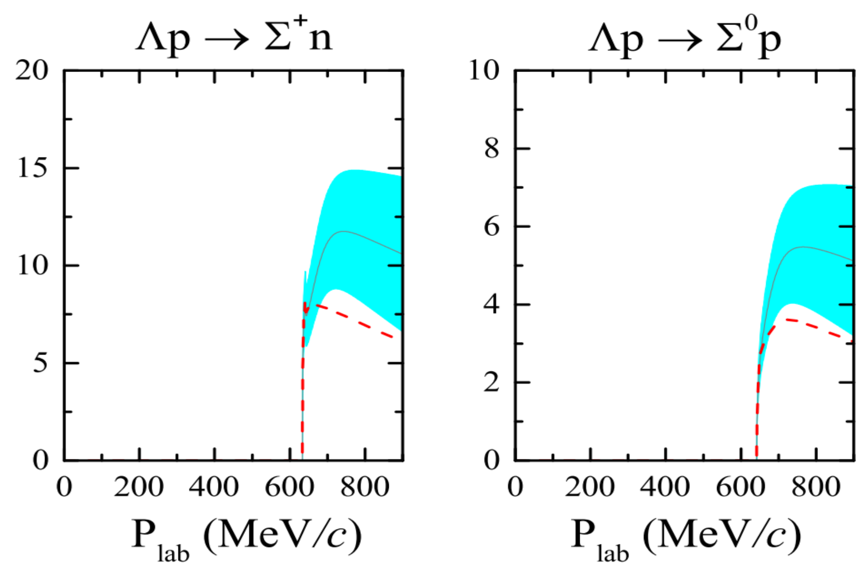

Study of $\Lambda p \to \Lambda p$ and $\bar{\Lambda} p \to \bar{\Lambda} p$

PRL 132, 231902 (2024)

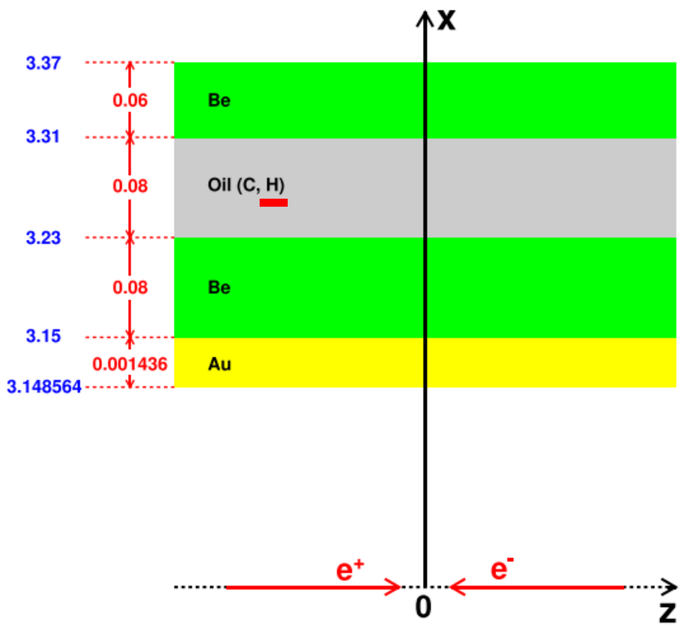

Taking the hydrogen in the cooling oil of the beam pipe as target material, the information on the hyperon-proton scattering can be extracted directly.

Two-body decay, $P_{\Lambda/\bar{\Lambda}} \approx 1.074\ \mathrm{GeV}/c$

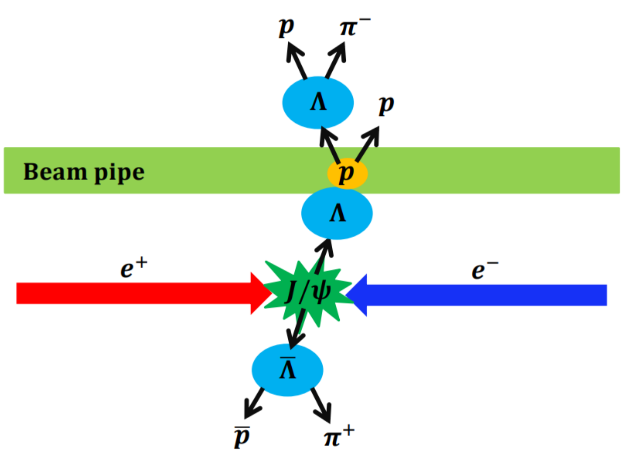

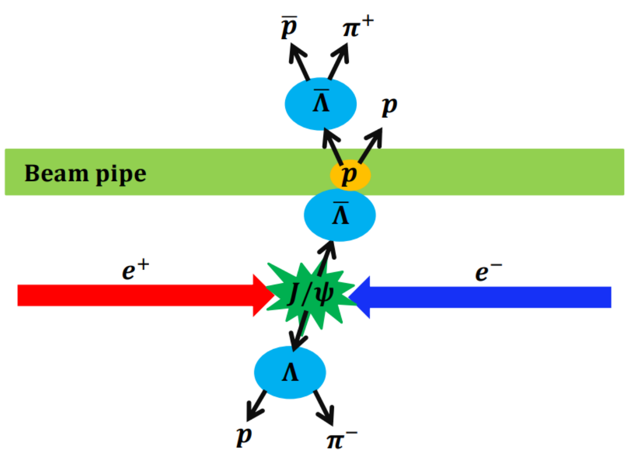

Study of $\Lambda p \to \Lambda p$ and $\bar{\Lambda} p \to \bar{\Lambda} p$

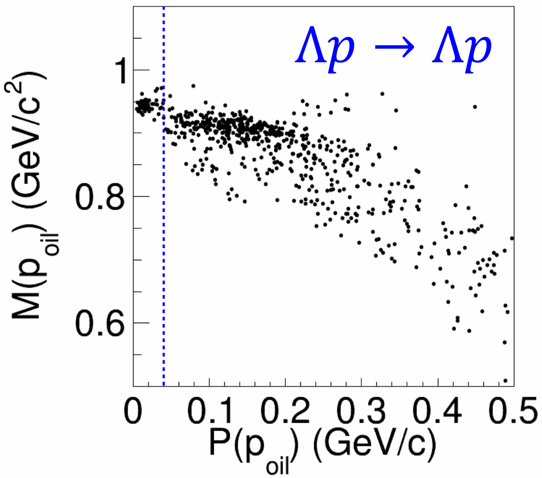

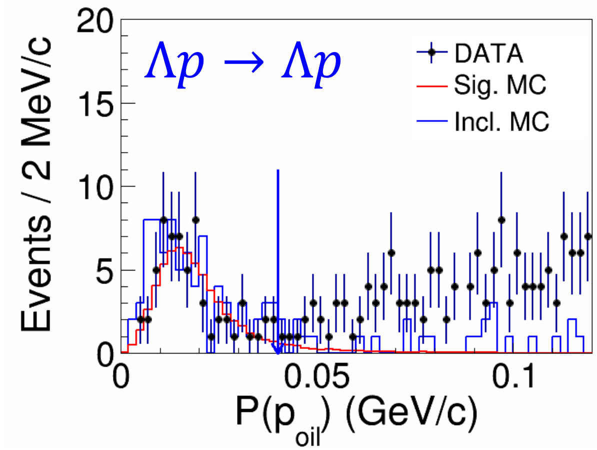

$J/\psi \to \Lambda\bar{\Lambda}$

$\Lambda p_{\text{oil}} \to \Lambda p$

$$P(p_{oil}) \equiv \left|\vec{P}_\Lambda + \vec{P}_p - \left(\vec{P}_{e^+e^-} - \vec{P}_{\bar{\Lambda}}\right)\right| < 0.04\ \text{GeV}/c$$

$$M(p_{oil}) \equiv \sqrt{|E_\Lambda + E_p - (E_{e^+e^-} - E_{\bar{\Lambda}})|^2 - |\vec{P}_\Lambda + \vec{P}_p - (\vec{P}_{e^+e^-} - \vec{P}_{\bar{\Lambda}})|^2}$$

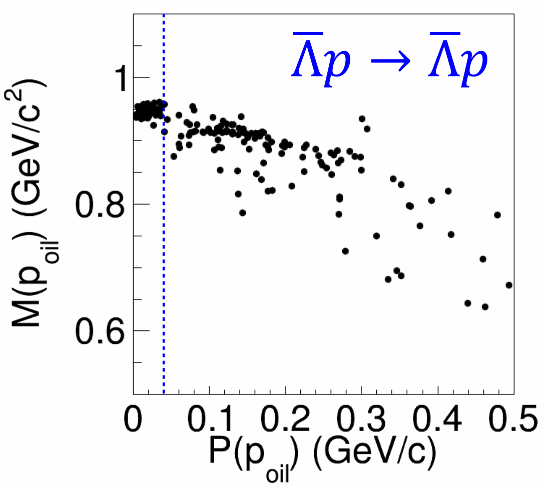

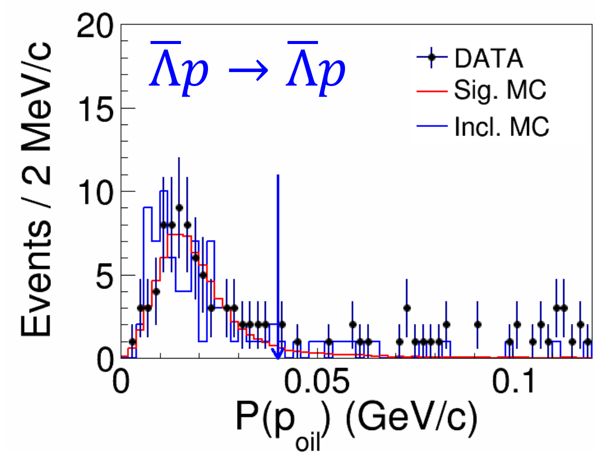

Study of $\Lambda p \to \Lambda p$ and $\bar{\Lambda} p \to \bar{\Lambda} p$

The center-of-mass energy for the incident $\Lambda/\bar{\Lambda}$ and a static p is about 2.243 GeV/c^2.

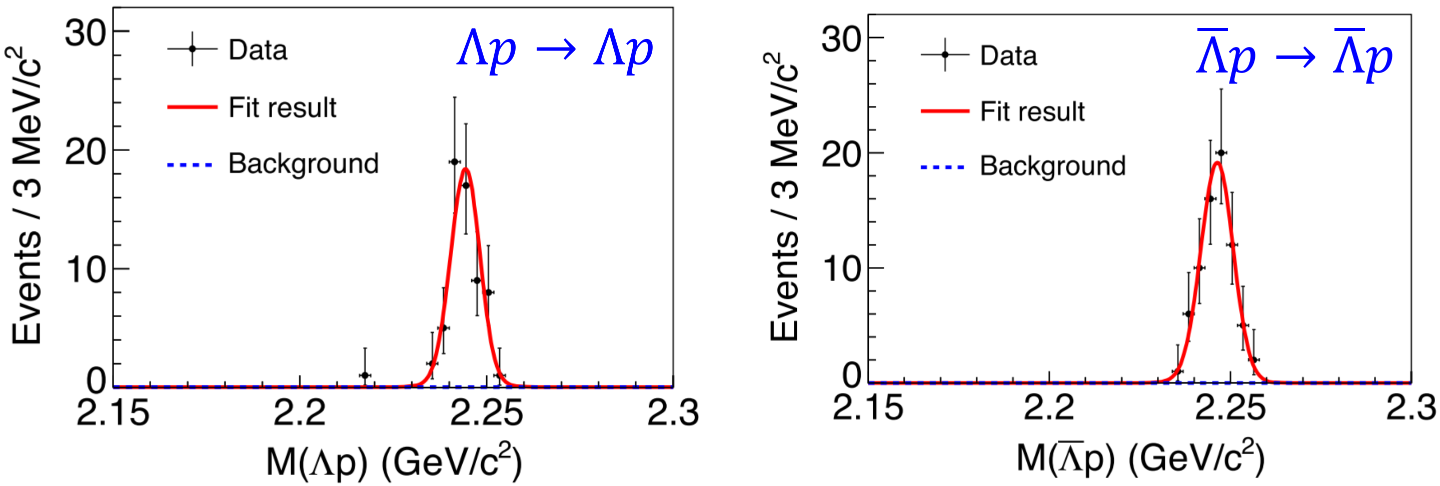

$$\sigma(\Lambda p \to \Lambda p/\bar{\Lambda} p \to \bar{\Lambda} p) = \frac{N^{\rm sig}_{\Lambda p/\bar{\Lambda} p}}{\epsilon_{\Lambda p/\bar{\Lambda} p}\mathcal{B}\mathcal{L}_{\rm eff}}$$

$$\left(\frac{d\sigma}{d\Omega}\right)_i = \frac{N_i^{\rm sig}}{\epsilon_i \mathcal{B}\mathcal{L}_{\rm eff}\Delta\Omega}$$

$$\mathcal{L}_{\rm eff} = \frac{N_{J/\psi}\mathcal{B}_{J/\psi}}{2+\frac{2}{3}\alpha}\int_a^b\int_0^\pi (1+\alpha\cos^2\theta)e^{-\frac{x}{\sin\theta\beta\gamma L}}N_H {\rm d}\theta{\rm d}x$$

Study of $\Lambda p \to \Lambda p$ and $\bar{\Lambda} p \to \bar{\Lambda} p$

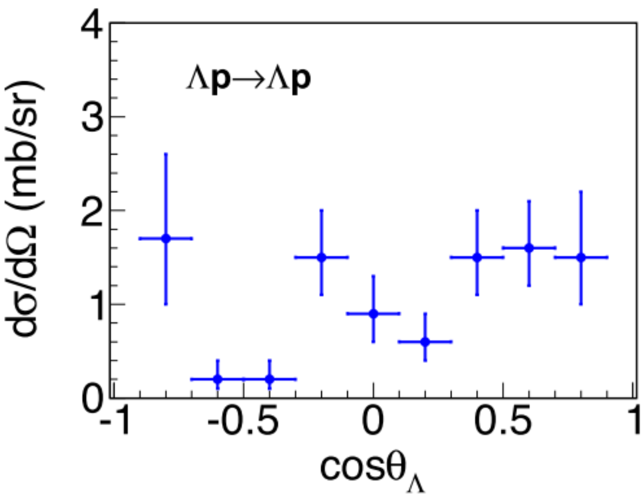

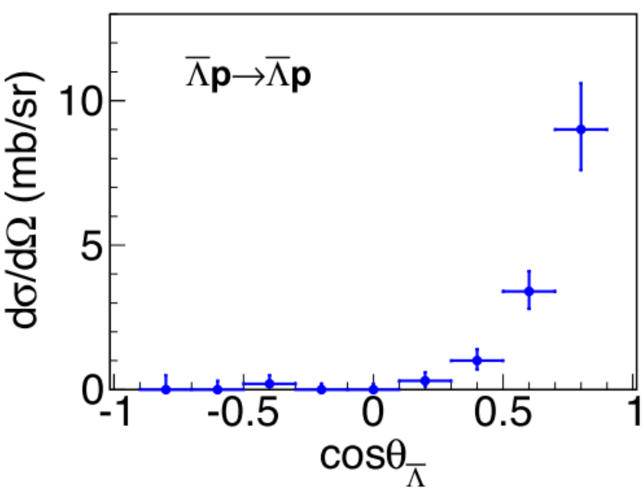

First measurement of antihyperon-nucleon scattering

$\cos\theta_{\Lambda/\bar{\Lambda}}$	N_i^{sig}	ϵ_i (%)	$(d\sigma/d\Omega)$ (mb/sr)
$[-0.9, -0.7]$	$(5.0^{+2.6}_{-1.9}, 0.0^{+1.1}_{-0.0})$	(6.94,4.93)	$(1.7^{+0.9}_{-0.7}, 0.0^{+0.5}_{-0.0})$
$(-0.7, -0.5]$	$(1.0^{+1.4}_{-0.7}, 0.0^{+1.1}_{-0.0})$	(14.13,10.44)	$(0.2^{+0.2}_{-0.1}, 0.0^{+0.3}_{-0.0})$
$(-0.5, -0.3]$	$(1.0^{+1.4}_{-0.7}, 1.0^{+1.4}_{-0.7})$	(17.32,13.27)	$(0.2^{+0.2}_{-0.1}, 0.2^{+0.3}_{-0.1})$
$(-0.3, -0.1]$	$(11.0^{+3.7}_{-3.0}, 0.0^{+1.1}_{-0.0})$	(17.74,14.66)	$(1.5^{+0.5}_{-0.4}, 0.0^{+0.2}_{-0.0})$
$(-0.1, 0.1]$	$(6.9^{+3.0}_{-2.3}, 0.0^{+1.1}_{-0.0})$	(19.11,15.79)	$(0.9^{+0.4}_{-0.3}, 0.0^{+0.2}_{-0.0})$
$(0.1, 0.3]$	$(5.0^{+2.6}_{-1.9}, 2.0^{+1.8}_{-1.1})$	(19.53,16.82)	$(0.6^{+0.3}_{-0.2}, 0.3^{+0.3}_{-0.2})$
$(0.3, 0.5]$	$(12.0^{+3.8}_{-3.1}, 7.0^{+3.0}_{-2.3})$	(19.21,17.68)	$(1.5^{+0.5}_{-0.4}, 1.0^{+0.4}_{-0.3})$
$(0.5, 0.7]$	$(13.0^{+3.9}_{-3.3}, 25.0^{+5.3}_{-4.7})$	(19.71,17.60)	$(1.6^{+0.5}_{-0.4}, 3.4^{+0.7}_{-0.6})$
$(0.7, 0.9]$	$(6.0^{+2.8}_{-2.1}, 37.0^{+6.4}_{-5.8})$	(9.80,9.93)	$(1.5^{+0.7}_{-0.5}, 9.0^{+1.6}_{-1.4})$

Cross sections in $-0.9 \le \cos\theta_{\Lambda/\bar{\Lambda}} \le 0.9$ are measured to be
$\sigma(\Lambda p \to \Lambda p) = (12.2 \pm 1.6_{\mathrm{stat}} \pm 1.1_{\mathrm{sys}})$ mb and
$\sigma(\bar{\Lambda} p \to \bar{\Lambda} p) = (17.5 \pm 2.1_{\mathrm{stat}} \pm 1.6_{\mathrm{stat}})$ mb

Total cross sections are determined to be
$\sigma_t(\Lambda p \to \Lambda p) = (14.2 \pm 1.8_{\mathrm{stat}} \pm 1.3_{\mathrm{sys}})$ mb and
$\sigma_t(\bar{\Lambda} p \to \bar{\Lambda} p) = (27.4 \pm 3.2_{\mathrm{stat}} \pm 2.5_{\mathrm{sys}})$ mb

Study of $\Lambda p \to \Lambda p$ and $\bar{\Lambda} p \to \bar{\Lambda} p$

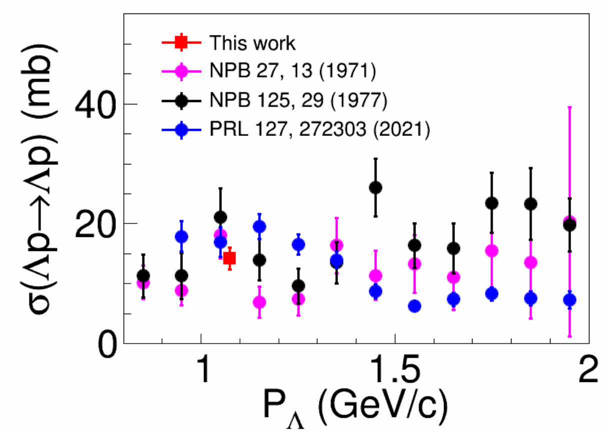

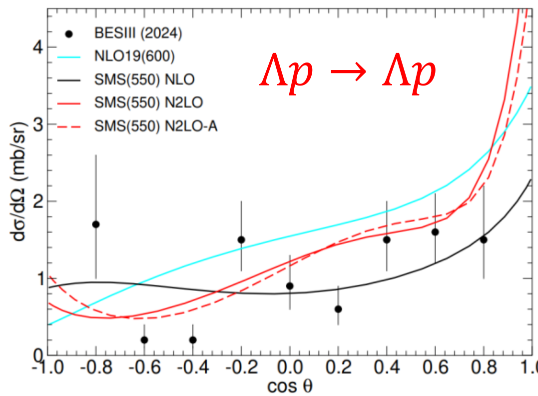

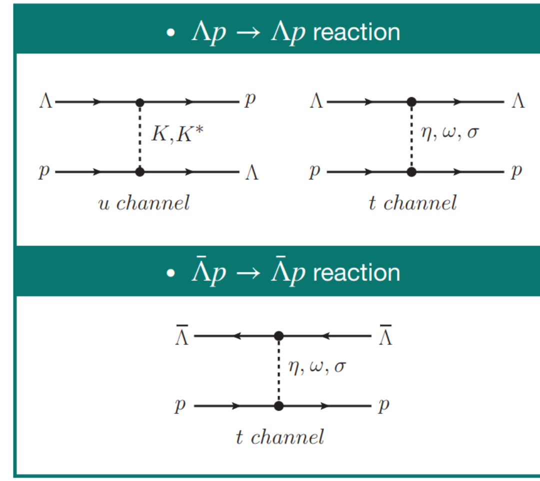

J. Haidenbauer and U. G. Meiβner, EPJA 60, 119 (2024)

X. Y. Wang, Y. Gao and X. Liu, PLB 862, 139321 (2025)

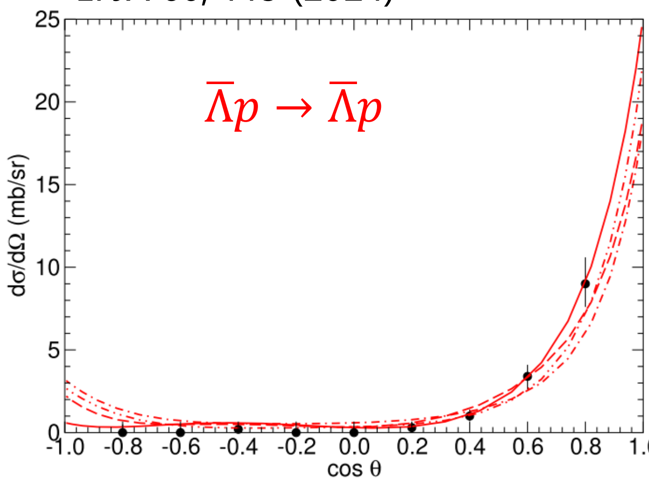

Fig. 1 Differential cross section for $p\bar{\Lambda}$ scattering at $p_{lab} = 1.074 \pm 0.017$ GeV [59]. The curves are predictions by the $\Lambda\bar{\Lambda}$ interactions I-IV, see Ref. [35], at 1.05 GeV/c

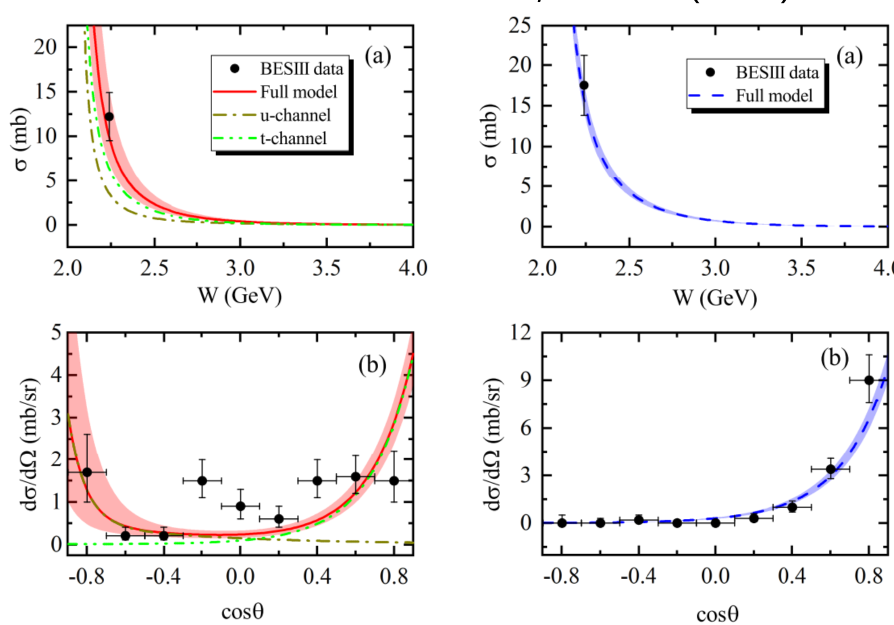

More (anti)hyperon-nucleon scattering can be studied at BESIII

Elastic scattering	Inelastic scattering
$\Lambda p \to \Lambda p$	$\Lambda p \to \Sigma^0 p,\ \Lambda p\pi^0,\ \Sigma^+ p\pi^-$
$\bar{\Lambda} p \to \bar{\Lambda} p$	$\bar{\Lambda} p \to \bar{\Sigma}^0 p,\ \bar{\Lambda} p\pi^0,\ \bar{\Sigma}^- p\pi^+$
$\Sigma^+ p \to \Sigma^+ p$	$\Sigma^+ p \to \Lambda p\pi^+,\ \Sigma^+ p\pi^0,\ \Sigma^0 p\pi^+$
$\bar{\Sigma}^- p \to \bar{\Sigma}^- p$	$\bar{\Sigma}^- p \to \bar{\Lambda} p\pi^-,\ \bar{\Sigma}^- p\pi^0,\ \bar{\Sigma}^0 p\pi^-$
$\Xi^0 p \to \Xi^0 p$	$\Xi^0 p \to \Lambda\Sigma^+,\ \Sigma^0\Sigma^+,\ \Xi^0 p\pi^0,\ \Xi^- p\pi^+$
$\bar{\Xi}^0 p \to \bar{\Xi}^0 p$	$\bar{\Xi}^0 p \to \bar{\Xi}^0 p\pi^0,\ \bar{\Xi}^+ p\pi^-$
$\Xi^- p \to \Xi^- p$	$\Xi^- p \to \Lambda\Lambda,\ \Lambda\Sigma^0,\ \Sigma^0\Sigma^0,\ \Xi^- p\pi^0,\ \Xi^0 p\pi^-$
$\bar{\Xi}^+ p \to \bar{\Xi}^+ p$	$\bar{\Xi}^+ p \to \bar{\Xi}^+ p\pi^0,\ \bar{\Xi}^0 p\pi^+$
$\Omega^- p \to \Omega^- p$	$\Omega^- p \to \Lambda\Xi^0,\ \Sigma^0\Xi^0,\ \Sigma^+\Xi^-$
$\bar{\Omega}^+ p \to \bar{\Omega}^+ p$	...

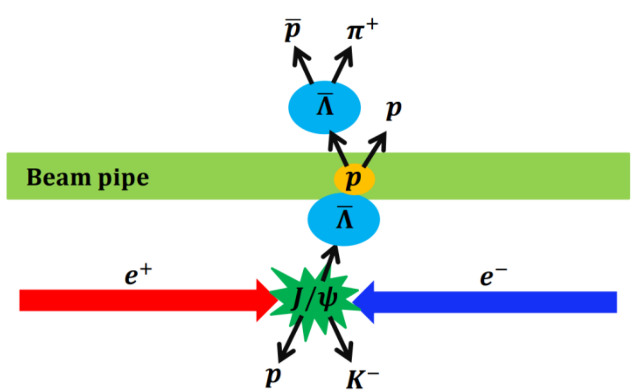

$\Lambda p \to \Lambda p/\bar{\Lambda} p \to \bar{\Lambda} p$ is studied using three-body decays $J/\psi \to pK\Lambda$, momentum-dependent cross section measurement.

Summary

1. Using a novel method, hyperon-nucleon scattering can also be measured at BESIII.
   - $\Xi^0 n \to \Xi^- p$
   - $\Lambda N \to \Sigma^+ X$
   - $\Lambda p \to \Lambda p$
   - $\bar{\Lambda} p \to \bar{\Lambda} p$

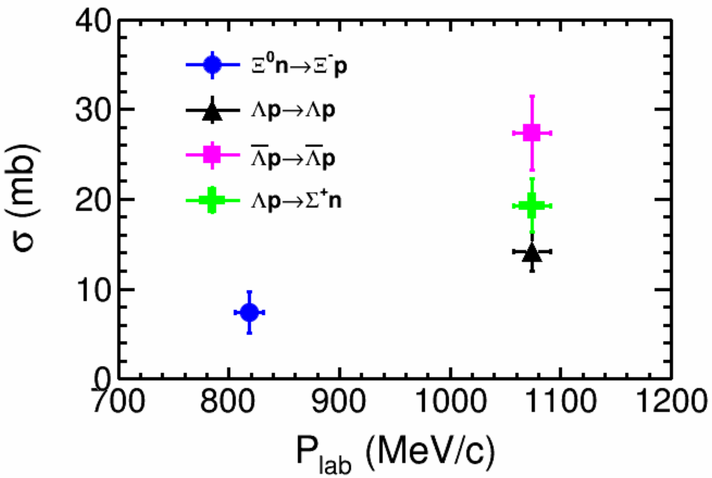

2. This is the first study of hyperon-nucleon interactions in electron-positron collisions, and opens up a new direction for such research. Especially, antihyperon-nucleon scattering is studied for the first time.

3. With more statistics in future super tau-charm facilities, the momentum-dependent cross section or differential cross section distributions can be studied based on the hyperons from multibody decays of J/ψ or other charmonia.

Thanks for your attention!

Back Up

Cross section measurement

A. Angular distribution of the process $J/\psi \to \Xi^0\bar{\Xi}^0$

The measured angular distribution of the process $J/\psi \to \Xi^0\bar{\Xi}^0$ in experiment is :

$$\frac{dN(\theta)}{d(\cos\theta)} \propto (1 + \alpha\cos^2\theta), \tag{1}$$

where $\cos\theta$ is from -1 to $+1$.

Because

$$\int_{-1}^{1} \frac{dN(\theta)}{d(\cos\theta)} d(\cos\theta) = N_{J/\psi}\mathcal{B}(J/\psi \to \Xi^0\bar{\Xi}^0), \tag{2}$$

we can get

$$\frac{dN(\theta)}{d(\cos\theta)} = \frac{N_{J/\psi}\mathcal{B}(J/\psi \to \Xi^0\bar{\Xi}^0)}{\int_{-1}^{1}(1 + \alpha\cos^2\theta)d(\cos\theta)}(1 + \alpha\cos^2\theta) = \frac{N_{J/\psi}\mathcal{B}(J/\psi \to \Xi^0\bar{\Xi}^0)}{2 + \frac{2}{3}\alpha}(1 + \alpha\cos^2\theta). \tag{3}$$

Therefore, the following formula can be obtained :

$$\frac{dN(\theta)}{d\theta} = \frac{N_{J/\psi}\mathcal{B}(J/\psi \to \Xi^0\bar{\Xi}^0)}{2 + \frac{2}{3}\alpha}(1 + \alpha\cos^2\theta)\sin\theta, \tag{4}$$

where θ is from 0 to π.

Cross section measurement

B. Number of the nuclei (Be, C, Au) per unit volume for beam pip

The beam pipe is composed of gold (Au), beryllium (Be) and oil (84.923%C, 15.077%H, C:H=1:2.13), as shown in Fig. 15. The distance from a position to the z axis is defined as x, so the number of the nuclei (Au, Be, C) per unit volume $N(x)$ is :

$$N(x) = \begin{cases} \frac{\rho_{\mathrm{Au}}}{A_{\mathrm{Au}}\cdot 1u} = \frac{19.32\mathrm{g/cm^3}}{197\cdot 1.6605\times 10^{-27}\mathrm{kg}} = 5.91\times 10^{22}\ \mathrm{cm^{-3}}, & 3.148564\ \mathrm{cm} \leq x \leq 3.15\ \mathrm{cm} \\ \frac{\rho_{\mathrm{Be}}}{A_{\mathrm{Be}}\cdot 1u} = \frac{1.85\mathrm{g/cm^3}}{9\cdot 1.6605\times 10^{-27}\mathrm{kg}} = 1.24\times 10^{23}\ \mathrm{cm^{-3}}, & 3.15\ \mathrm{cm} < x \leq 3.23\ \mathrm{cm} \\ \frac{\rho_{\mathrm{Oil}}}{(A_{\mathrm{C}}+A_{\mathrm{H}}\cdot 2.13)\cdot 1u} = \frac{0.81\mathrm{g/cm^3}}{(12+1\cdot 2.13)\cdot 1u} = 3.45\times 10^{22}\ \mathrm{cm^{-3}}, & 3.23\ \mathrm{cm} < x \leq 3.31\ \mathrm{cm} \\ \frac{\rho_{\mathrm{Be}}}{A_{\mathrm{Be}}\cdot 1u} = \frac{1.85\mathrm{g/cm^3}}{9\cdot 1.6605\times 10^{-27}\mathrm{kg}} = 1.24\times 10^{23}\ \mathrm{cm^{-3}}, & 3.31\ \mathrm{cm} < x \leq 3.37\ \mathrm{cm} \end{cases} \quad (5)$$

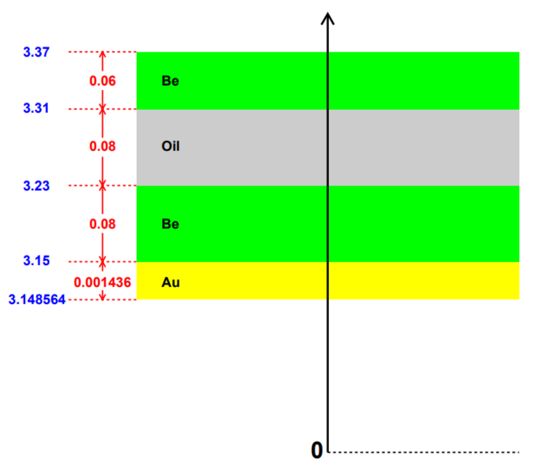

Figure 15: The sketch map of beam pip, the length units are centimeter (cm). The solid line is x-axis, and the dashed line is z-axis.

Cross section measurement

C. Ratio of cross section of $\Xi^0 + {}^{A}X \to \Xi^- + p + {}^{A-1}X$ for Be, C and Au nuclei

There is no definite conclusion about the ratio of cross section of reaction process $\Xi^0 + {}^{A}\mathrm{X} \to \Xi^- + p + {}^{A-1}\mathrm{X}$ for Be, C and Au nuclei. Generally, from the measurements of other particles interact with nuclei, the cross section is proportional to A^{α}, where A is the number of nucleon in the nuclei and α is about from $\frac{2}{3}$ to 1 [45, 46, 47]. $\alpha = \frac{2}{3}$ is the most common situation, which is corresponding to a pure surface process and the reaction is due to the interaction with single nucleon on the nuclei surface.

Here for the reaction process $\Xi^0 + {}^{A}\mathrm{X} \to \Xi^- + p + {}^{A-1}\mathrm{X}$, we also assume the $\alpha = \frac{2}{3}$ to get the ratio of cross section for Be, C and Au nuclei. We assume the reaction is due to the interaction with single neutron on the nuclei surface, which is a pure surface process. So the cross section is proportional to $A^{\frac{2}{3}} \times \frac{N}{A} = \frac{N}{A^{\frac{1}{3}}}$, where A is the number of nucleons and N is the number of neutron. We can get $\sigma^{\mathrm{Be}} : \sigma^{\mathrm{C}} : \sigma^{\mathrm{Au}} = \frac{5}{9^{\frac{1}{3}}} : \frac{6}{12^{\frac{1}{3}}} : \frac{118}{197^{\frac{1}{3}}} = 2.4037 : 2.6207 : 20.2796 = 1 : 1.090 : 8.437$. We define $\sigma(x) = C(x)\sigma^{\mathrm{Be}} = C(x)\sigma(\Xi^0 + {}^{9}\mathrm{Be} \to \Xi^- + p + {}^{8}\mathrm{Be})$, where $C(x)$ is :

$$C(x) = \begin{cases} 8.437, & 3.148564\ \mathrm{cm} \le x \le 3.15\ \mathrm{cm} \\ 1, & 3.15\ \mathrm{cm} < x \le 3.23\ \mathrm{cm} \\ 1.090, & 3.23\ \mathrm{cm} < x \le 3.31\ \mathrm{cm} \\ 1, & 3.31\ \mathrm{cm} < x \le 3.37\ \mathrm{cm} \end{cases} \quad (6)$$

$\alpha = \frac{2}{3}$

Phys. Rev. D 27, 2580 (1983)

Z. Phys. C 76, 35 (1997)

Nucl. Phys. A 697, 209 (2002)

$\sigma \propto A^{\alpha}$

α is about $\frac{2}{3} \sim 1$.

We use $\alpha = 1$ to estimate the systematic uncertainty.

Cross section measurement

D. Efficiency curve $\epsilon(x)$

The average efficiency in beam pipe region is determined to be $\epsilon = 18675/997312 = (1.873 \pm 0.014)\%$.

The beam pipe region is small, so we can take the efficiency in beam pipe region as a constant. Therefore, the efficiency curve is $\epsilon(x) = 1.873\%$.

E. Cross section of the reaction process $\Xi^0 + {}^9\text{Be} \rightarrow \Xi^- + p + {}^8\text{Be}$

As shown in Fig. 16, at the position of θ and within the range of $d\theta$, the number of Ξ^0 that can reach the position of x is :

$$\frac{dN(\theta)}{d\theta} d\theta e^{-\frac{t}{\tau}\sqrt{1-\frac{v^2}{c^2}}} = \frac{dN(\theta)}{d\theta} d\theta e^{-\frac{x}{\sin\theta v \tau}\sqrt{1-\frac{v^2}{c^2}}} = \frac{dN(\theta)}{d\theta} d\theta e^{-\frac{x}{\sin\theta \frac{P}{m}\tau}} = \frac{dN(\theta)}{d\theta} d\theta e^{-\frac{x}{\sin\theta \frac{\sqrt{E^2-m^2c^4}}{mc^2} L}}, \qquad (7)$$

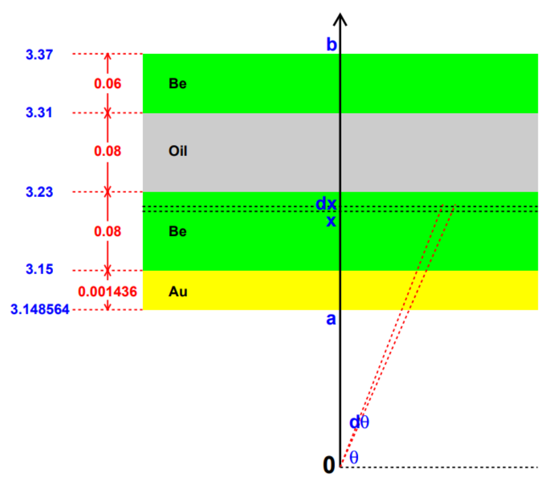

Figure 16: The sketch map of beam pip, the length units are centimeter (cm). The solid line is x-axis, and the dashed line is z-axis.

Cross section measurement

Then these Ξ^0 particles interact with neutron n in the target material in the dx range at x position to produce the reaction process $\Xi^0 + n \to \Xi^- + p$. So the number of signal events survived for the reaction process is :

$$\frac{dN(\theta)}{d\theta} d\theta e^{-\frac{x}{\sin\theta \frac{\sqrt{E^2-m^2c^4}}{mc^2} L}} \sigma(x) N(x) \frac{dx}{\sin\theta} \epsilon(x) \mathcal{B}, \tag{8}$$

where $\mathcal{B} = \mathcal{B}(\bar{\Xi}^0 \to \bar{\Lambda}\pi^0)\mathcal{B}(\bar{\Lambda} \to \bar{p}\pi^+)\mathcal{B}(\pi^0 \to \gamma\gamma)\mathcal{B}(\Xi^- \to \Lambda\pi^-)\mathcal{B}(\Lambda \to p\pi^-)$.

So the total number of signal events N^{sig} survived for the reaction process is :

$$N^{\text{sig}} = \int_a^b \int_0^\pi \frac{N_{J/\psi}\mathcal{B}(J/\psi \to \Xi^0\bar{\Xi}^0)}{2 + \frac{2}{3}\alpha}(1 + \alpha\cos^2\theta) e^{-\frac{x}{\sin\theta \frac{\sqrt{E^2-m^2c^4}}{mc^2} L}} \sigma(x) N(x) \epsilon(x) \mathcal{B} d\theta dx. \tag{9}$$

Therefore, the cross section formula of $\Xi^0 + {}^9\text{Be} \to \Xi^- + p + {}^8\text{Be}$ is :

$$\sigma(\Xi^0 + {}^9\text{Be} \to \Xi^- + p + {}^8\text{Be}) = \frac{N^{\text{sig}}}{\frac{N_{J/\psi}\mathcal{B}(J/\psi \to \Xi^0\bar{\Xi}^0)\mathcal{B}}{2+\frac{2}{3}\alpha} \int_a^b \int_0^\pi (1 + \alpha\cos^2\theta) e^{-\frac{x}{\sin\theta \frac{\sqrt{E^2-m^2c^4}}{mc^2} L}} C(x) N(x) \epsilon(x) d\theta dx}, \tag{10}$$

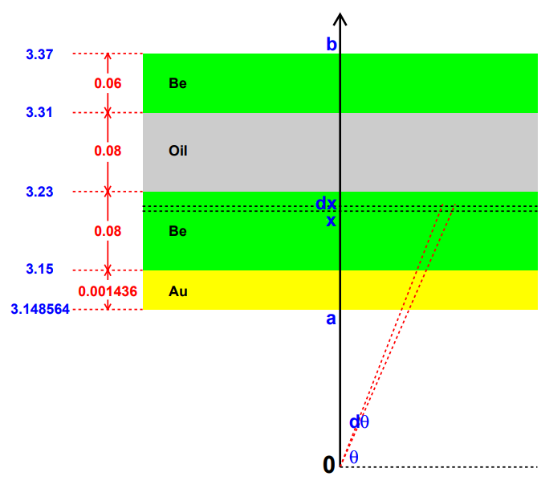

Figure 16: The sketch map of beam pip, the length units are centimeter (cm). The solid line is x-axis, and the dashed line is z-axis.

Signal MC for $\Lambda p \to \Lambda p$

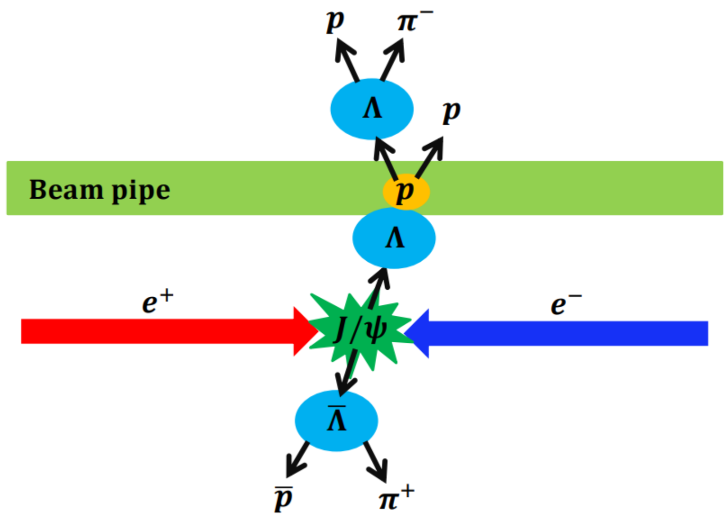

Signal MC :

$e^+e^- \to \mathrm{X}\bar{\Lambda}$,

$\mathrm{X} \to \Lambda p$,

$\Lambda \to p\pi^-$,

$\bar{\Lambda} \to \bar{p}\pi^+$.

The properties of particle X are same as those of Λ except for mass. The X mass is set to be $2.243\ \mathrm{GeV}/c^2$, which is center-of-mass energy for Λ and static p. And only the events where the position of X decays is in hydrogen region of beam pipe are used.

To guarantee the $\bar{\Lambda}$ momentum is same as actual one. The e^+e^- energy is set to be

$$E_{e^+e^-} = \sqrt{P_{\bar{\Lambda}}^2 c^2 + m_{\bar{\Lambda}}^2 c^4} + \sqrt{P_{\bar{\Lambda}}^2 c^2 + m_{\mathrm{X}}^2 c^4}.$$

Some distributions

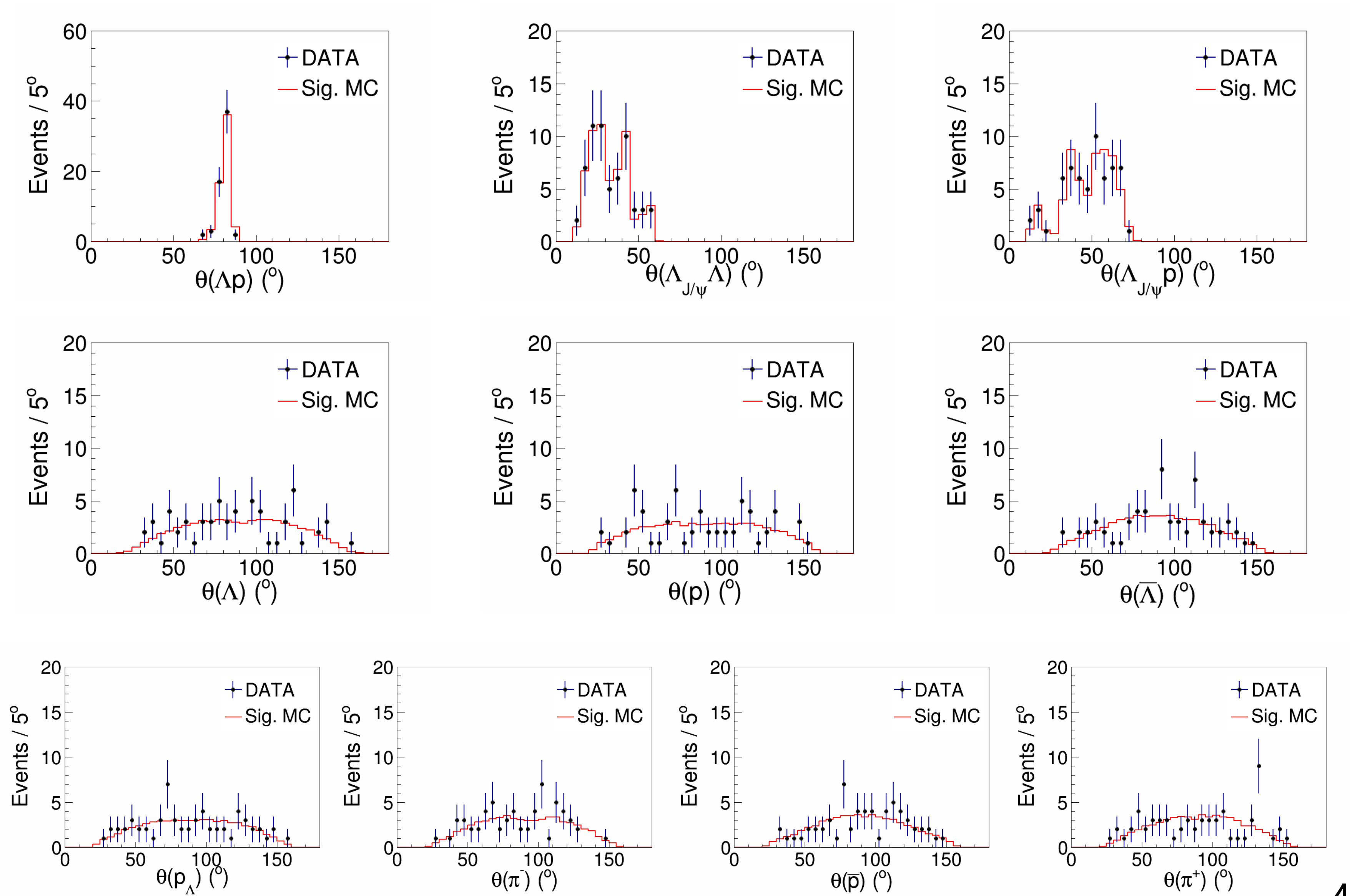

Some distributions

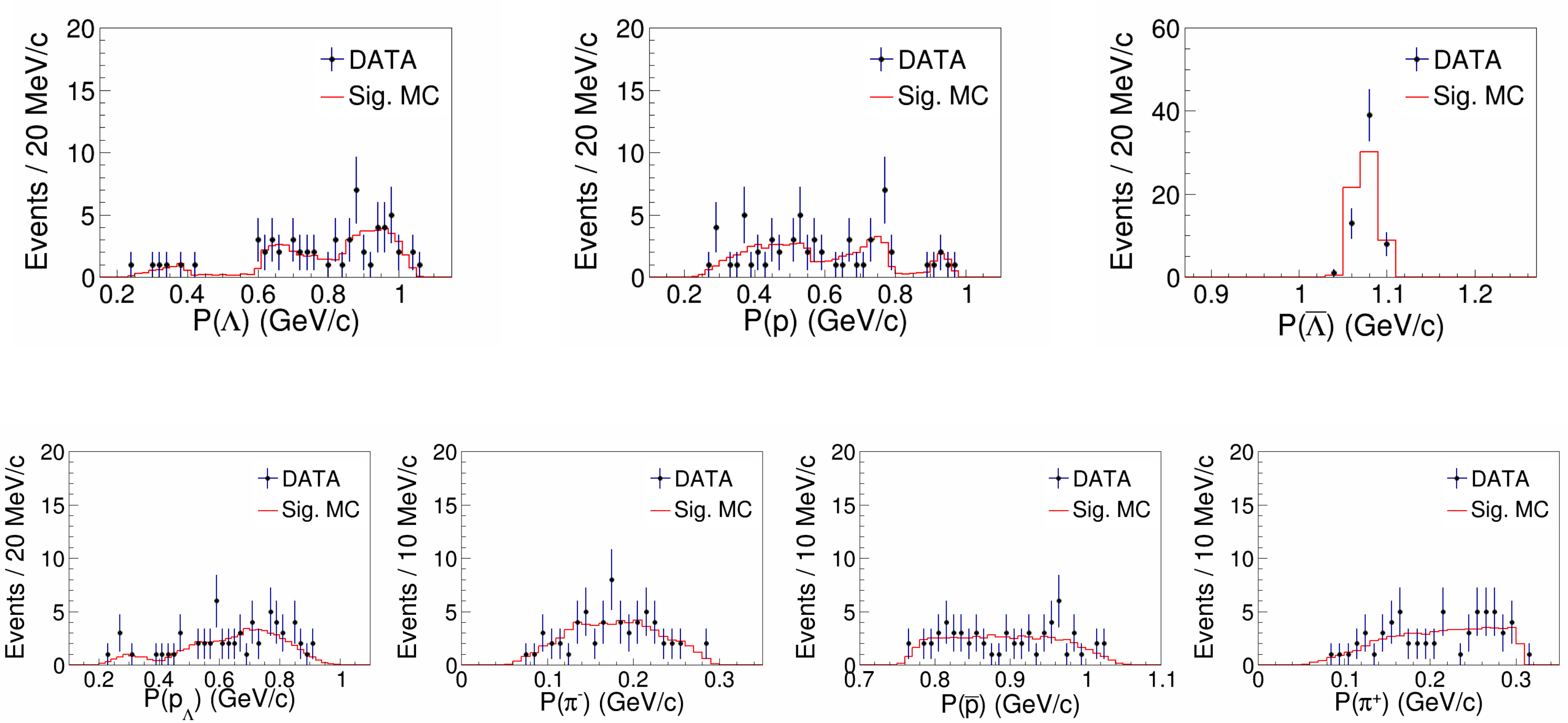

Some distributions

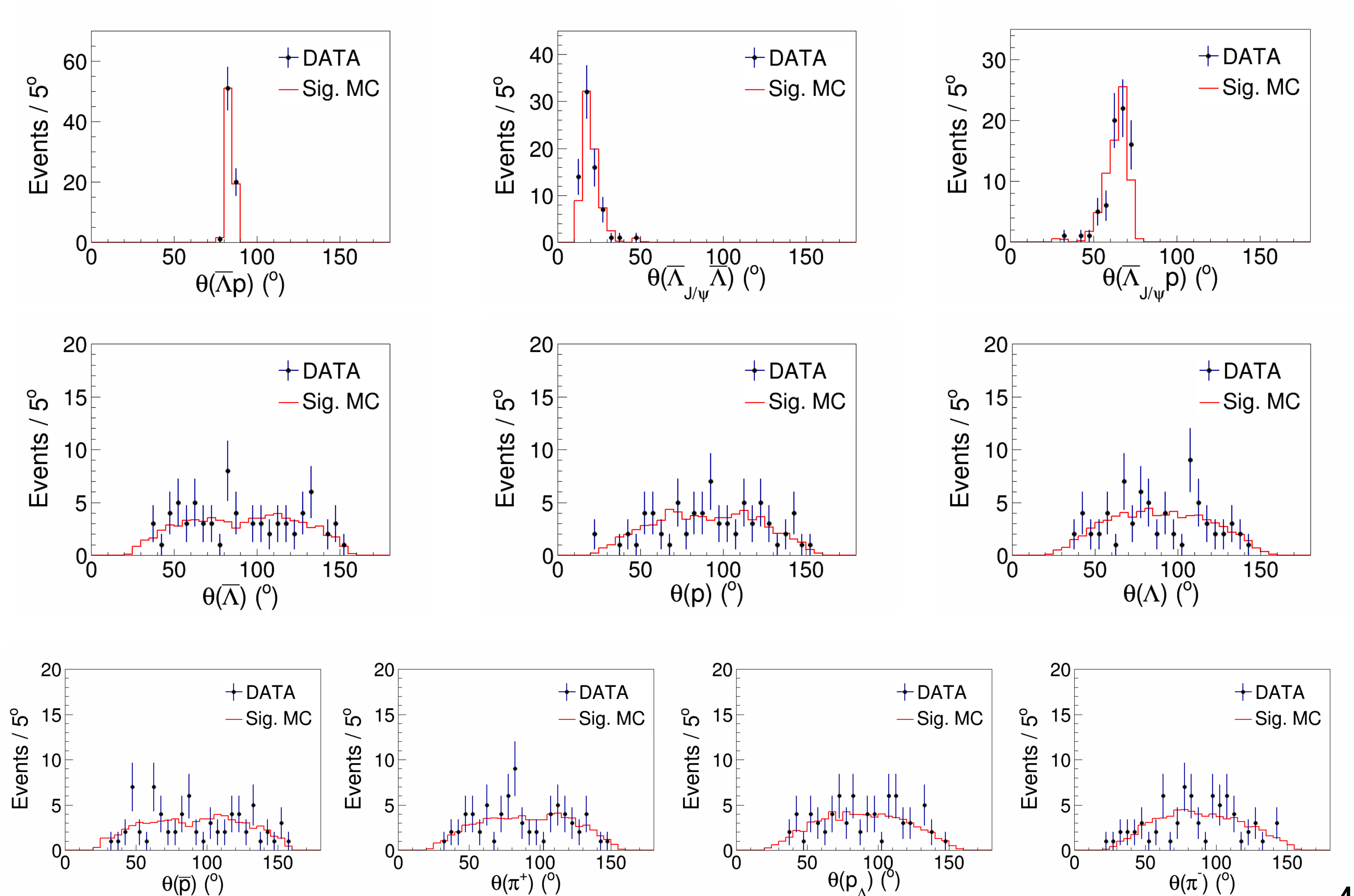

Some distributions